M.R.P. 956
S.C. 11/204
23rd January, 1956

# The use of a stream function in the Sawyer - Bushby two parameter model of the atmosphere

by

F. H. Bushby and Vera M. Huckle
(Meteorological Office)

AIR MINISTRY
METEOROLOGICAL RESEARCH COMMITTEE

At the time of issue this report has not been published. Any author desiring to quote this paper should refer to it as "A paper of the Meteorological Research Committee (London).
M.R.P. No. 956 by Mr. F. H. Bushby and Mrs. V. M. Huckle
A copy is available in the Library of the Meteorological Office."

M.R.P. 956
S.C.II/204
23rd January, 1956

AIR MINISTRY

METEOROLOGICAL RESEARCH COMMITTEE

# The use of a stream function in the Sawyer - Bushby two parameter model of the atmosphere

by
F. H. Bushby and Vera M. Huckle (Meteorological Office)

## 1. Introduction

Most of the recent work on numerical weather prediction has been characterized by the use of the geostrophic approximation to the wind field. An examination of about twenty computed forecasts based on the Sawyer-Bushby (1) two parameter model of the atmosphere suggested that in one or two situations the use of the geostrophic approximation was possibly responsible for a large part of the difference between computed and actual charts.

This paper describes an attempt to improve upon the geostrophic approximation by representing the wind field in an isobaric surface by a stream function which differs from the geopotential. The stream function is derived from an equation similar to the balance equation derived by Charney (2) which relates the horizontal velocity field at a given pressure level with the contours of the same isobaric surface. Three 24-hr. forecasts have been computed applying this technique to the two parameter model and the results compared with previous computations in which no attempt had been made to improve upon the geostrophic approximation.

## 2. The derivation of the stream function

Since the significant motions of the free atmosphere are characterized by small horizontal divergences we can adequately express the velocity components u and v in terms of a stream function $\phi$ by

$$u = -\frac{g}{l}\frac{\partial \phi}{\partial s} \quad , \quad v = \frac{g}{l}\frac{\partial \phi}{\partial r} \qquad \text{---- (1)}$$

where r and s are orthogonal curvilinear distance co-ordinates on the sphere. If the rather slow variation of the Coriolis parameter l with latitude is ignored, this velocity field is non-divergent.

Ignoring the vertical motion terms and the variations of l, substituting from Eq. (1) and taking the horizontal divergence of the equations of motion, we obtain (when pressure is used as the vertical co-ordinate),

$$\frac{2g}{l^2}\left\{\left(\frac{\partial^2\phi}{\partial r\,\partial s}\right)^2 - \frac{\partial^2\phi}{\partial r^2}\frac{\partial^2\phi}{\partial s^2}\right\} - \nabla_e^2\phi = -\nabla_e^2 h \qquad \text{---- (2)}$$

where h is the height of the contour surface and $\nabla_e^2$ is the two-dimensional Laplacian operator on the sphere. This equation is of the Monge-Ampère type and can be solved for $\phi$ as a boundary value problem provided that

$$g\frac{\nabla^2 h}{l} + \frac{l}{2} > 0 .$$

In the analysis given by Charney (2) he does not need to ignore the variation of the Coriolis parameter with latitude as he uses a stream function such that

$$u = -\frac{\partial \phi}{\partial s} \qquad v = \frac{\partial \phi}{\partial r} \qquad \text{---- (3)}$$

Charney then derives an equation similar to Eq. (2) but including a term grad $\phi$ grad l. Although Charney's equation can be derived with one less approximation than Eq. (2), it is more difficult to obtain suitable boundary values for $\phi$ when Eq. (3) is used to define the stream function than if Eq. (1) is used for that purpose.

Representing the earth's surface by a stereographic projection of the northern hemisphere on to a plane perpendicular to the earth's axis passing through the north pole, Eq. (2) becomes approximately

$$2\,\frac{\beta^2 g}{l^2}\left\{\left(\frac{\partial^2\phi}{\partial x\,\partial y}\right)^2 - \frac{\partial^2\phi}{\partial x^2}\cdot\frac{\partial^2\phi}{\partial y^2}\right\} - \nabla^2\phi = -\nabla^2 h \qquad \text{---- (4)}$$

where $\beta$ is the magnification factor $\sec^2(\pi/4 - \theta/2)$ and x and y are the rectangular Cartesian co-ordinates on the plane. The ratio of the small terms neglected in deriving Eq. (4) from Eq. (2) to the smallest terms which appear in Eq. (4) is of the same order as the ratio of the wavelength of the characteristic patterns of the stream function to the circumference of the earth.

Eq. (4) can be written as the following finite difference approximation:-

$$\sum_1^4 \phi_i - 4\phi_0 + 4h_0 - \sum_1^4 h_i - \frac{2\beta_0^2 g}{a^2 l_0^2}\left\{\frac{1}{16}(\phi_A + \phi_C - \phi_B - \phi_D)^2 - (\phi_1 + \phi_3 - 2\phi_0)(\phi_2 + \phi_4 - 2\phi_0)\right\} = 0 \qquad \text{---- (5)}$$

where a = grid length and the suffixes refer to points relative to the origin O as shown in Fig. 4. Eq. (5) is a quadratic equation in $\phi_0$ and can be re-written as

$$\phi_0 = \frac{4K + 2\Sigma\phi_i \pm \sqrt{16K^2 + 4(\Sigma\phi_i)^2 + 16Ka^2\nabla^2 h + (\phi_A + \phi_C - \phi_B - \phi_D)^2 - 16(\phi_1 + \phi_3)(\phi_2 + \phi_4)}}{8} \qquad \text{---- (6)}$$

where $K = \dfrac{a^2 l_0^2}{2\beta_0^2 g}$ .

It is clear that the solution we require is the one with the negative sign outside the square root; e.g., consider the case of parallel equidistant straight contour lines.

Given $\phi$ on the boundary we can obtain a solution to Eq. (5) by making an initial guess at the answer (say $\phi = h$) and then using Eq. (6) in a systematic point to point manner over the grid, continuing the process until there is no longer any significant change in $\phi$. Since the stream function is defined by Eq. (1) it is possible to use $\phi = h$ on the boundary as the boundary condition. The iterative process is slowly convergent. 15 to 20 iterations were usually needed to obtain the necessary accuracy in the answer when an 18 x 14 grid was used.

The above procedure is not possible if the quantity under the radical (say A) in Eq. (6) is negative. In practice this difficulty was overcome by replacing a negative A by zero. If we consider a stream function $\phi$ consisting of a series of concentric circles then A not negative implies $\frac{2}{l}\nabla^2 h + \frac{1}{2} \gg 0$, the condition necessary for Eq. (2) to be solved as a

/boundary

boundary value problem. With circular isobars this is equivalent to the condition that the actual absolute vorticity must not be negative.

3. Application of the stream function to the two parameter model

We can represent the horizontal velocity by a stream function only if the flow is approximately non-divergent, and therefore it would appear difficult to make use of a stream function in any model other than the simple barotropic one.

However the two parameters $h_m$, $h'$ of the Sawyer-Bushby model refer to the height of the mean level of the layer considered and the thickness of the layer. $h_m$ is used solely to represent the flow at the mean level (which even in the two parameter model is thought to be approximately non-divergent, consistent with the assumption of a parabolic vertical motion profile) and we therefore decided to replace $h_m$ by $\phi_m$ in the prognostic equations. $h'$ however, besides representing the wind shear, does in fact represent the mean temperature of the layer, and it was therefore decided to leave the parameter $h'$ unaltered.

Three time integrations were performed in which $\phi_m$ was first computed from the initial $h_m$, $\phi_m$ was subsequently used instead of $h_m$ during the time integration, and finally $h_m$ at time t = 24 was computed from $\phi_m$ at that time by solving Eq. (5) as a Poisson equation for $h_m$ given $\phi_m$ and boundary values for $h_m$. The boundary values of $h_m$ were taken as $h_m = \phi_m$.

The particular form of the Sawyer-Bushby model used for this experiment was the one which took 600 mb. as the mean level of the layer, included the effect of sea surface heating and used the actual changes that occurred on the boundary as boundary conditions. The results have been compared with time integrations not using the stream function but otherwise using the same version of the two parameter model.

4. The results of the time integration

(a) 1500 GMT 27 January, 1952.

The computation for this situation without use of the stream function has been discussed by Bushby and Hinds (3). Figs. 1a - 1d show the actual charts at the beginning and end of the period. The computed charts not using and using the stream function are also shown in Figs. 1e - 1h.

The introduction of the stream function has made little difference to the forecast charts. At the 500 mb. level a closed circulation has been introduced over Scandinavia, but the position and central values are not very accurate. Over most of the area the introduction of the stream function has led to a reduction in the height of the 500 mb. level by something of the order of 100 - 200 ft. This is not an improvement on the earlier computation and may have been brought about by a reduction in the total anticyclonic vorticity in the forecast area as a result of replacing a negative A by zero.

It is evident by comparing charts 1f and 1h that the use of the stream function has only had a slight effect on the thickness. Thus the difference between the two computed 1000 mb. charts is almost the same as the difference between the computed 500 mb. charts.

(b) 1500 GMT 30 January, 1952.

Although previous computations had been made for this situation they had been made with other variations of the Sawyer-Bushby model than that used here. (Bushby and Hinds (3) and (4)). Thus it is important to note that when this variation is used (without stream function) there are certain differences from the previous numerical forecasts. The trough from south of Iceland to the Faroes now turns down over the eastern North Sea (Fig. 2e) rather than continuing eastwards over Norway and Sweden and there is now

no cut-off 500 mb. depression in the vicinity of the Faroes. The axis of the jet is now west-east over the British Isles. The thickness and 1000 mb. patterns (Fig. 2f) are also slightly different from those produced in previous numerical forecasts.

The results of the calculations using the stream function technique are given in Figs. 2g and 2h. The 500 mb. trough is now forecast to be over the western North Sea which is better than the forecast without the stream function. Also, the axis of the jet stream is further south although still not far enough and is orientated west north west - east south east. Fig. 2e shows pronounced ridging over the southwestern seaboard of Europe whereas this is minimised to a large extent in Fig. 2g.

Again there is only very little difference between the computed thickness charts shown in Figs. 2f and 2h, and the improvement in the 1000 mb. pattern in Fig. 2h compared with the 1000 mb. chart shown in Fig. 2f is similar to that already described relative to the 500 mb. pattern.

(c) 1500 GMT 30 January, 1953.

The synoptic situation in the vicinity of the British Isles at this time (Figs. 3a and 3b) is of particular interest because within 24 hours large areas of east and southeast England and the Low Countries were being affected by a severe gale and coastal flooding was the worst for many years.

Numerical integrations previously performed on this data (Bushby and Hinds (3, 4)) had used 500 mb. as the level representing the mean tropospheric flow and had used no change on the boundary as the boundary condition. In these earlier computations the main features producing the gale had been indicated quite well, but an anticyclone west of Ireland had been grossly exaggerated, leading to too strong wind gradients over the British Isles.

Figs. 3e and 3f show the result of a time integration which used the 600 mb. level to represent the mean flow and which used the actual changes round the boundary as the boundary condition. These charts show a marked improvement west of Ireland where the intensity of the surface anticyclone is much more realistic and almost correct, but an upper closed anticyclonic circulation is still wrongly forecast (although it is much weaker than in the previous computations) southwest of Ireland. The trough over the North Sea is still broadly correct at 500 mb., although the main trough line is now too far west and in this respect the previous computations were better, both at the 500 mb. level and at the surface where the strong northerly winds are computed too far west over the British Isles. However, the position and intensity of the depression between Scotland and Norway (Fig. 3d) is almost exactly forecast.

The result of using the stream function technique in this particular situation is shown in Figs. 3g and 3f. The upper anticyclonic circulation has now almost completely disappeared, and the region west of Ireland is now correctly dealt with apart from the fact that the contour heights along the axis of the ridge are about 200 ft. too low. This again is probably due to the fact that a negative A is replaced by zero, thus giving less anticyclonic geostrophic vorticity in the forecast area than there should be. The fact that this is not replaced at the end of the computation when the $h_m$ field is computed from the $\phi_m$ field does imply that the mean value of $h_m$ inside the forecast area is less than it should be. This again probably accounts for the depression east of Scotland being a little too deep in Fig. 3h.

/In

In this particular situation a somewhat better answer (apart from the position of the 500 mb. trough line near the British Isles) has been obtained by using 600 mb. rather than 500 mb. as the operative level and by using the actual changes along the boundary rather than assuming no change along the boundary. The introduction of the stream function technique has made a further slight improvement in the forecast in the anticyclonic region west of Ireland.

## 5. Conclusions

This experiment has shown that it is quite practicable to carry out the solution of the Monge-Ampère equation on an electronic computing machine by using the iterative procedure described in Section 2. The use of the stream function technique extends the length of the computation from about $3\frac{1}{2}$ hours to 4 hours on the Manchester University electronic computer.

Apart from a systematic tendency to produce lower forecast values than actually occurred due to an initial reduction of the total anticyclonic geostrophic vorticity in the forecast area, there was no indication in any of the three situations examined that the use of the stream function made the computed forecast worse. In the first situation there was little difference in the forecasts with and without the stream function. On the other two occasions the computed forecasts using the stream function were better than the corresponding forecasts without the stream function.

It is impossible to decide on the basis of the three situations so far examined whether or not it would be desirable to extend the length of the computation by 10% in order to make use of the stream function in the two parameter model in the crude manner described in this paper. Nevertheless the authors believe that in cases of strong winds the technique described in this paper would often make a significant improvement in the forecast, whereas in other cases it would make little difference.

## 6. References


1. Sawyer, J.S. and Bushby, F.H. 1953 J. Met., 10, p. 54.
2. Charney, J. 1955 Tellus, 7, No. 1.
3. Bushby, F.H. and Hinds, M.K. 1955 Quart. J. R. Met. Soc., 81, No. 349.
4. Bushby, F.H. and Hinds, M.K. 1954 Meteorological Research Papers, Air Ministry, London, No. 863.

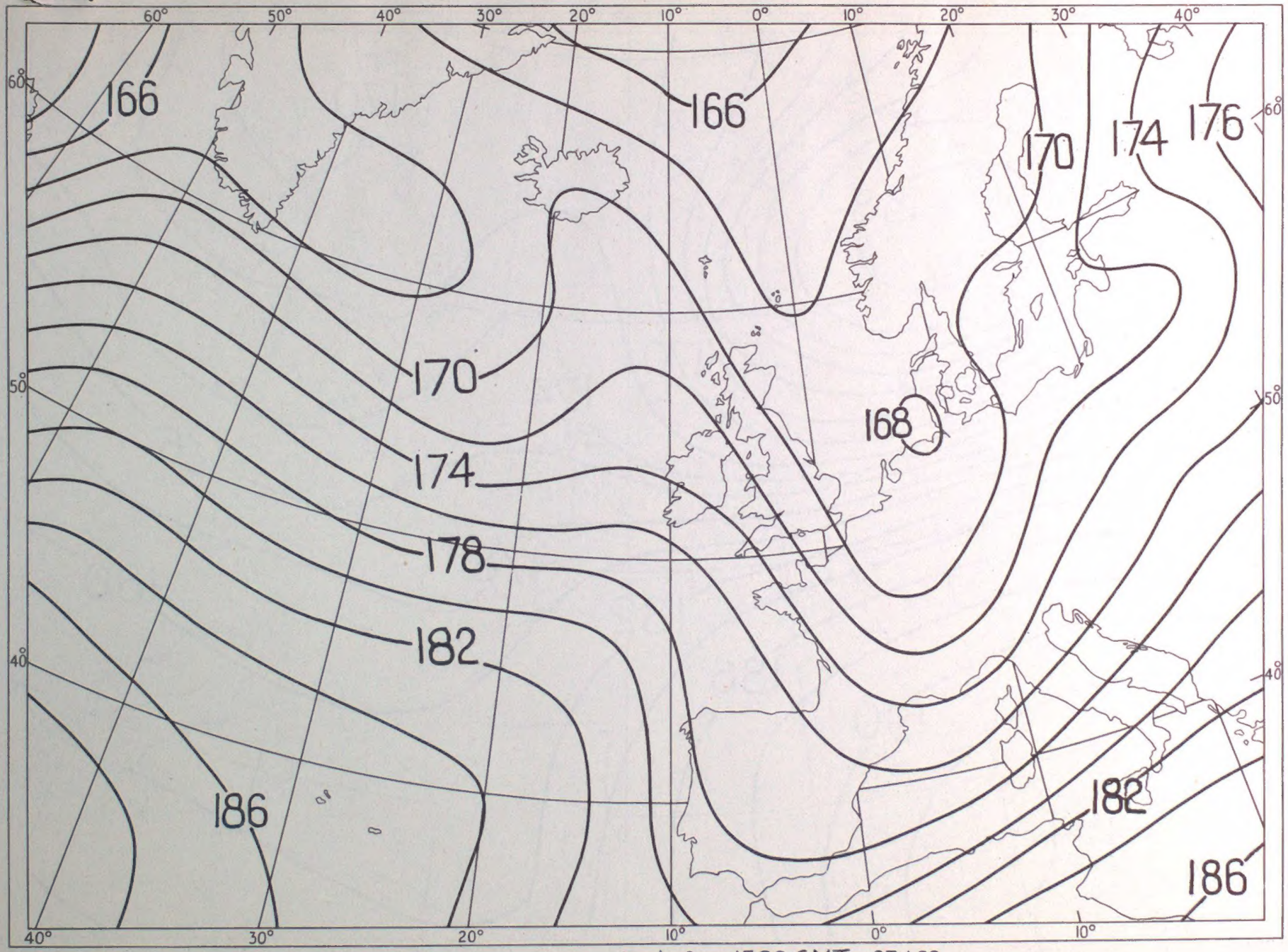


Fig 1(a) Actual 500mb. contour chart for 1500 G.M.T. 27:1:52

M.R.P. 956

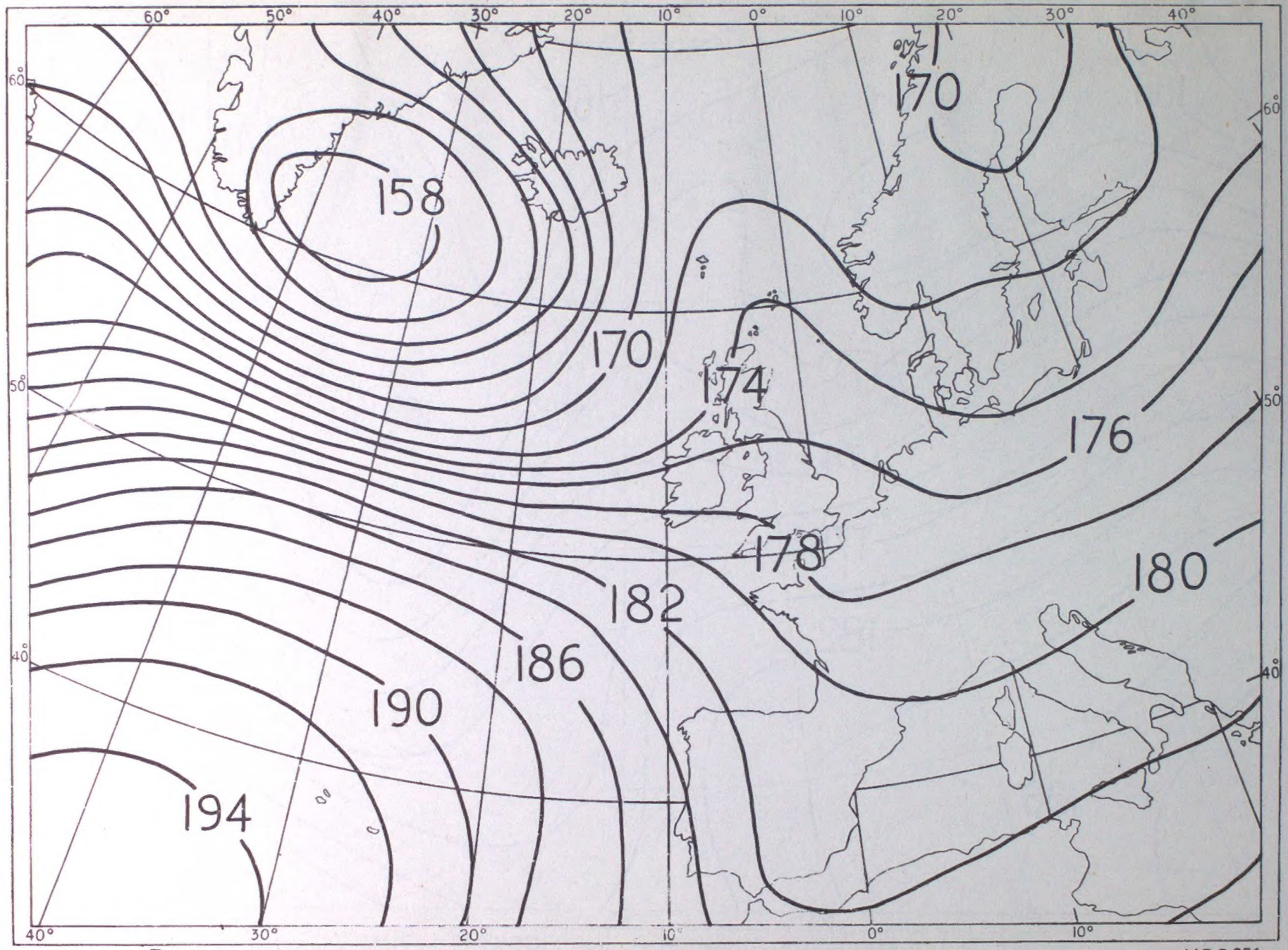


Fig.2(a) Actual 500mb. contour chart for 1500 G.M.T. 30.1.52

M.R.P. 956

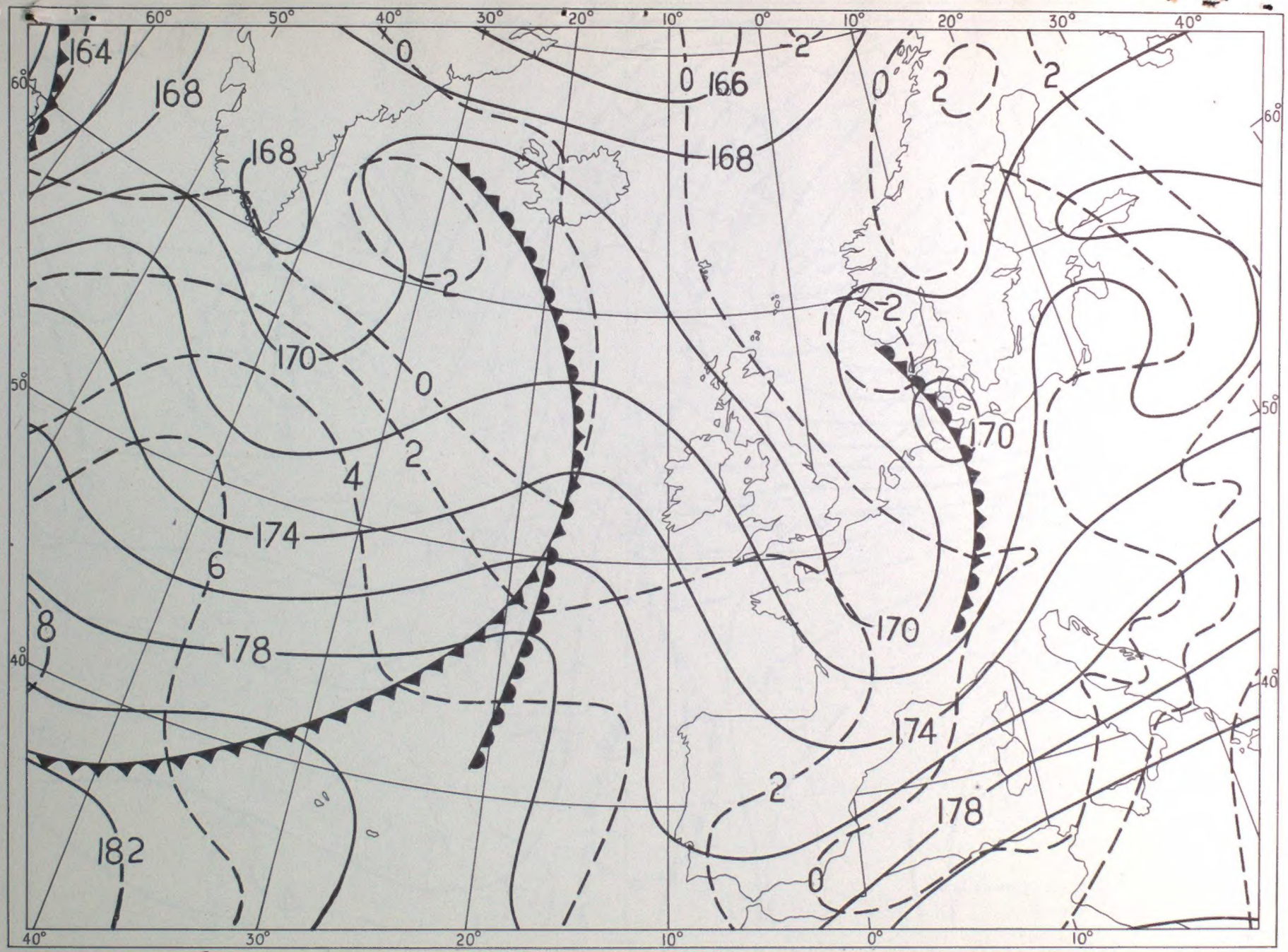


Fig. 1(b) Actual 1000-500mb. thickness and 1000mb. contour charts for 1500 G.M.T. 27:1:52

M.R.P. 956

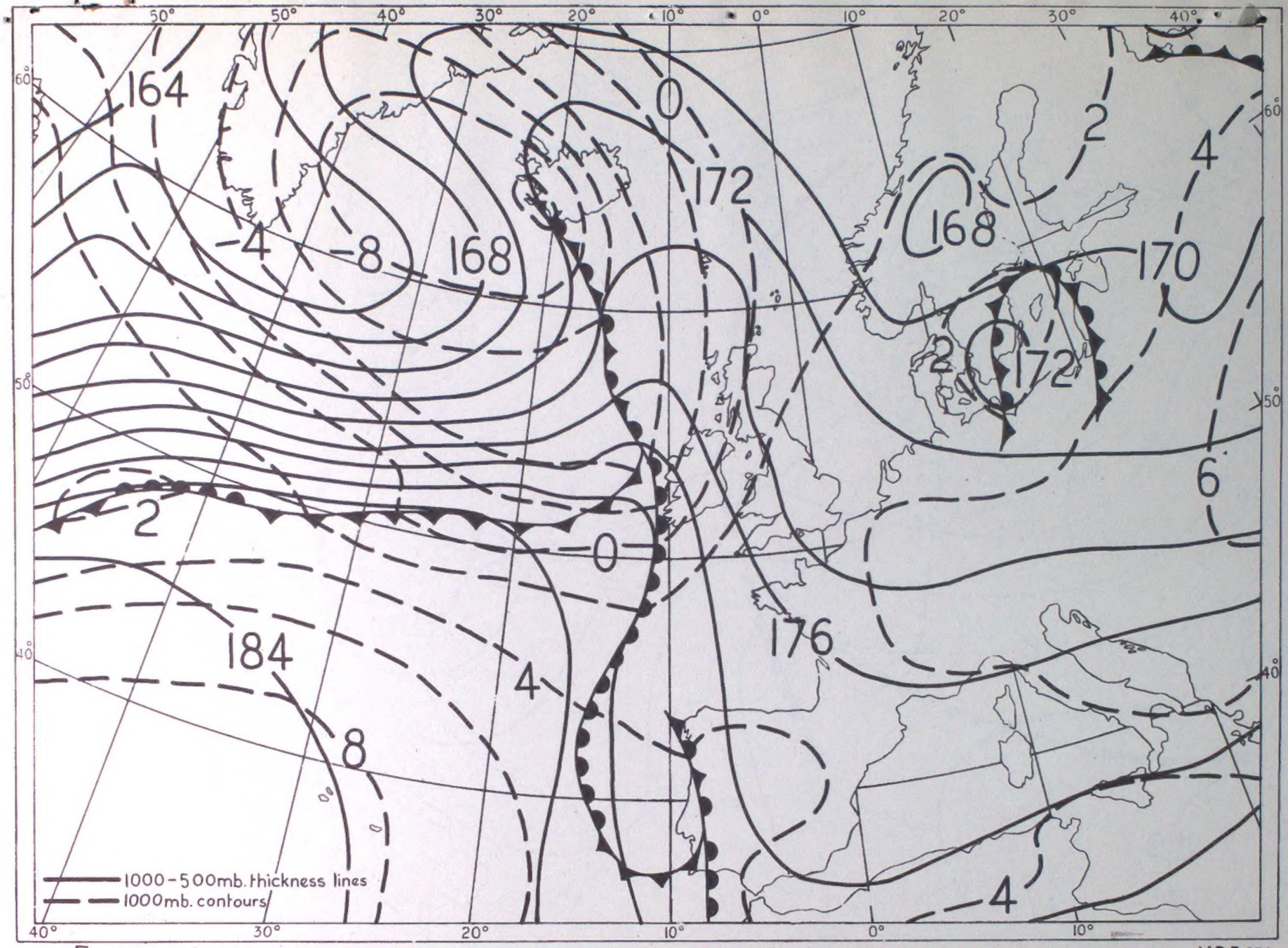


Fig.2(b) Actual 1000-500mb. thickness and 1000mb. contour charts for 1500 G.M.T. 30.1.52

M.R.P. 956

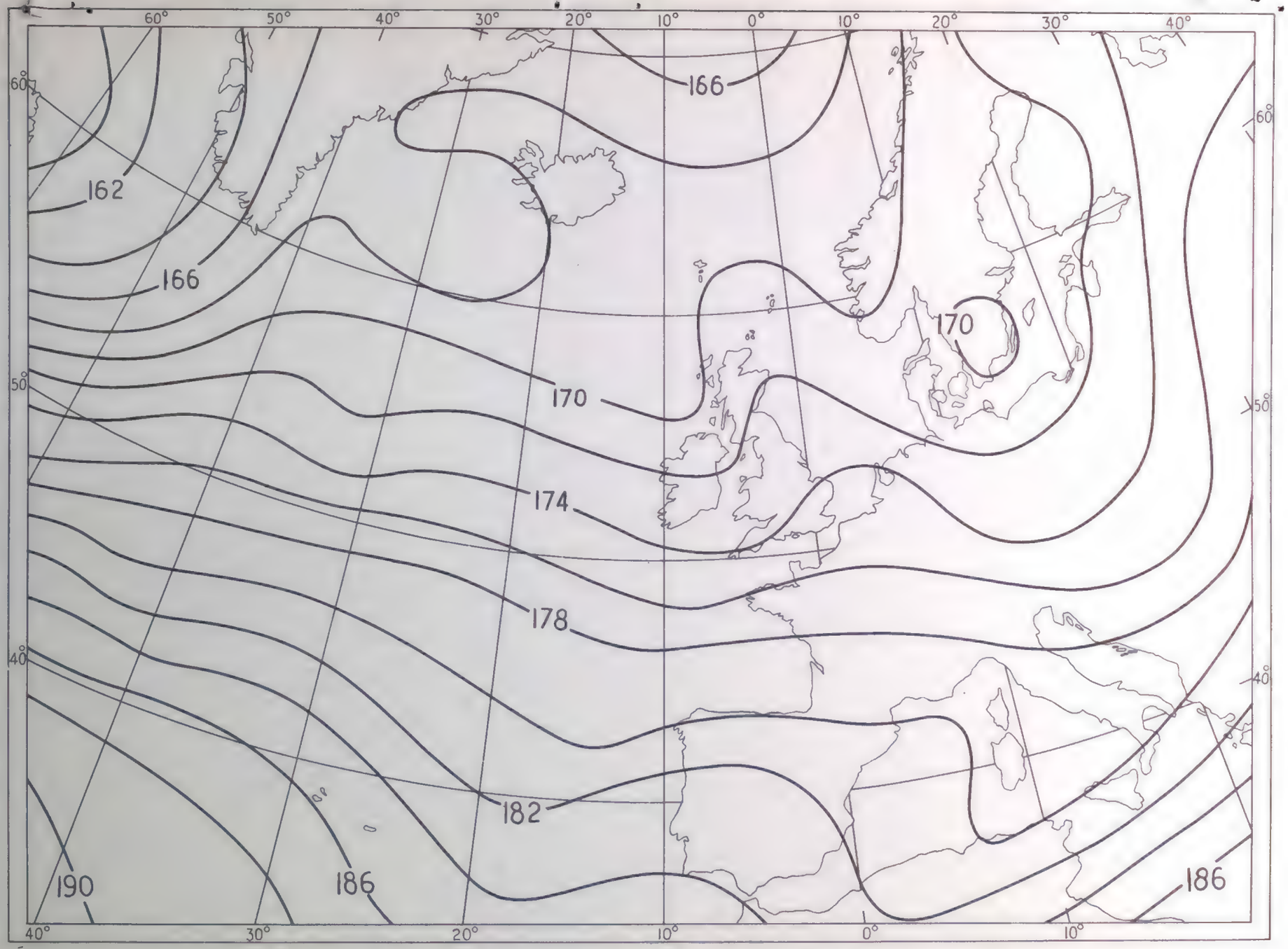


Fig 1(c) Actual 500 mb contour charts for 1500 G.M.T. 28:1:52

M.R.P. 956

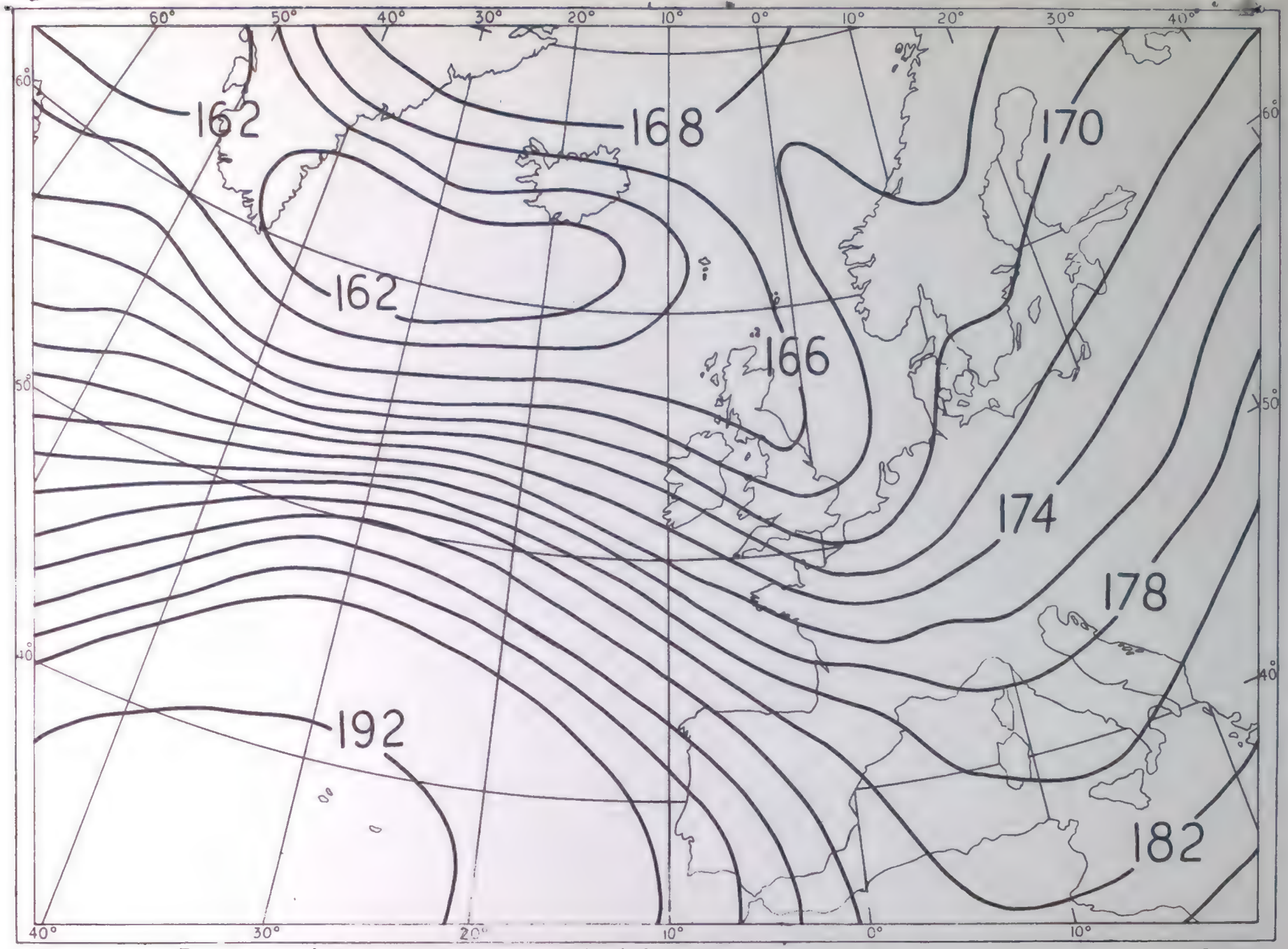


Fig.2(c) Actual 500mb. contour chart for 1500 G.M.T. 31.1.52

M.R.P. 956

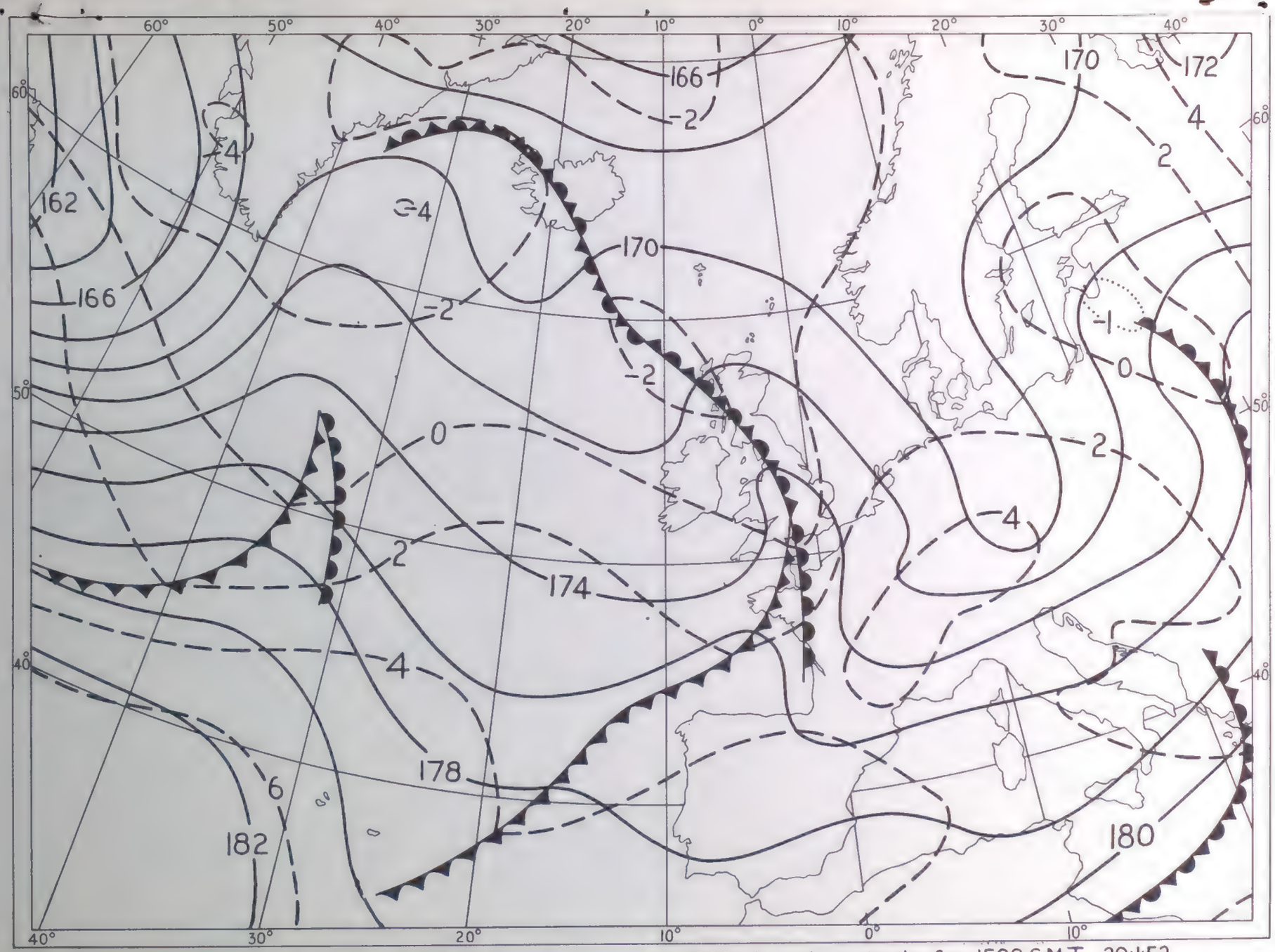


Fig 1(d) Actual 1000-500mb. thickness and 1000mb. contour charts for 1500 G.M.T 28:1:52

M.R.P. 956

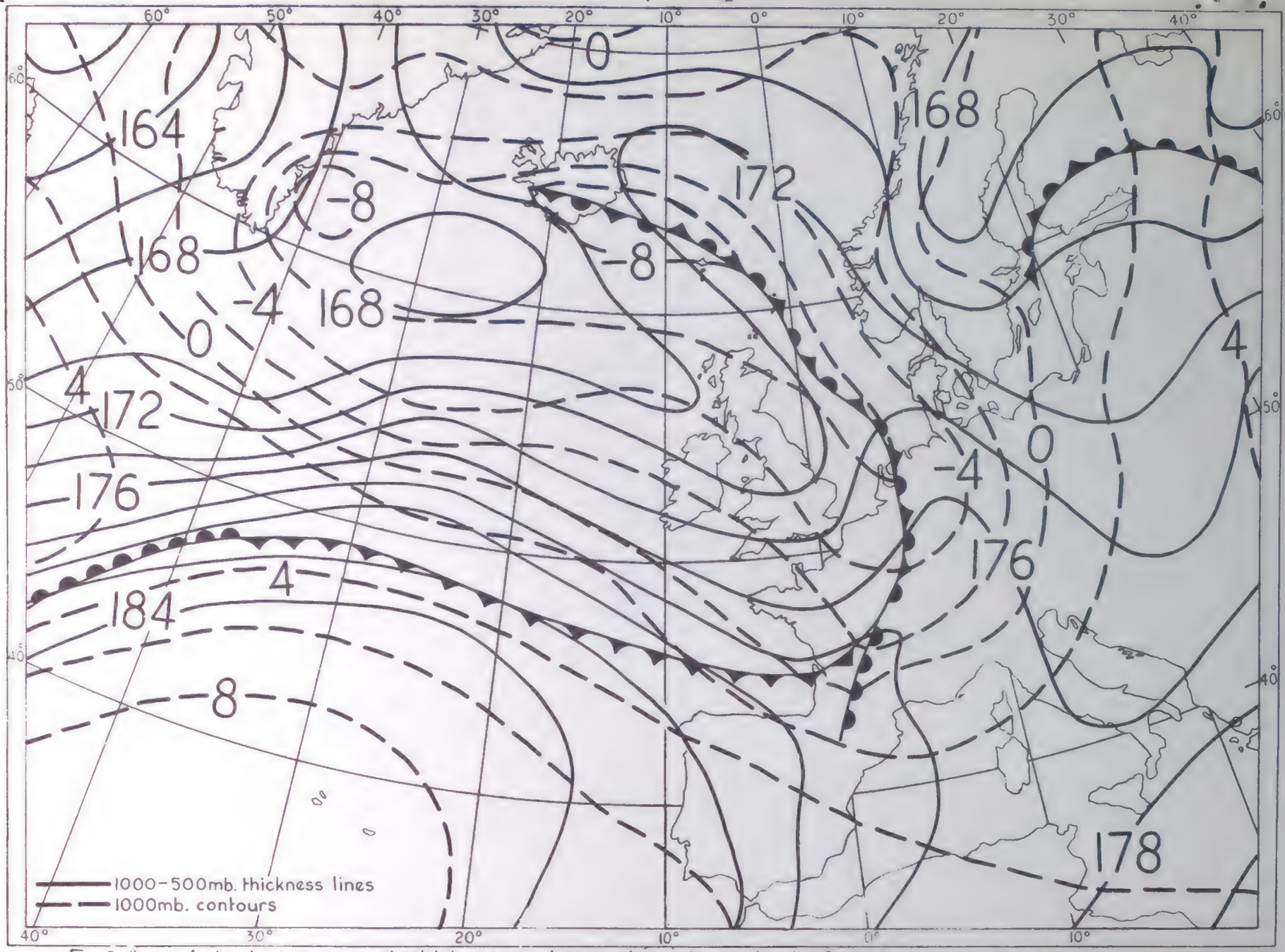


Fig.2(d) Actual 1000-500mb. thickness and 1000mb. contour charts for 1500 G.M.T. 31.1.52

M.R.P. 956

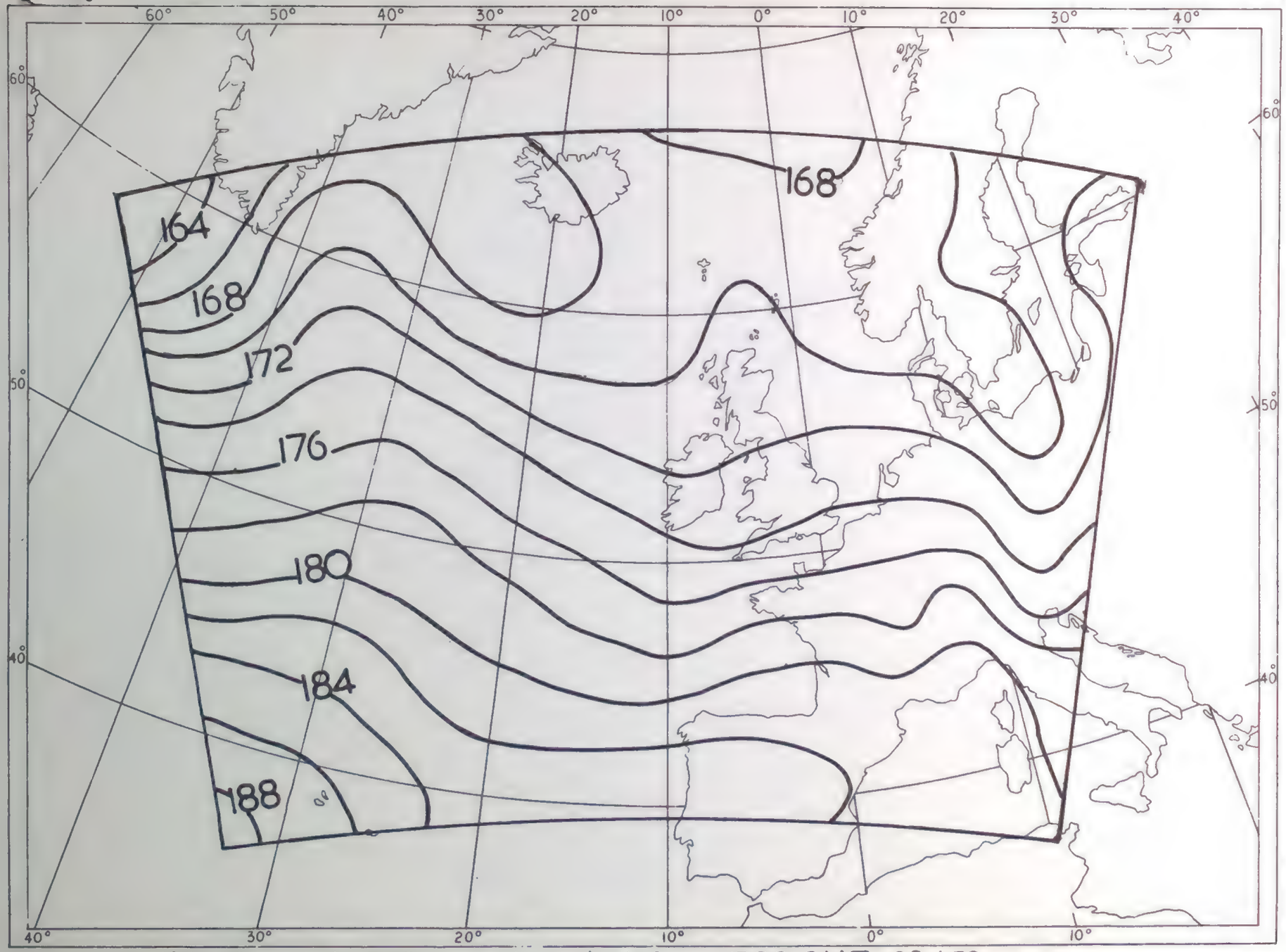


Fig. 1(e) Computed 500mb. contour chart for 1500 G.M.T. 28:1:52

M.R.P. 956

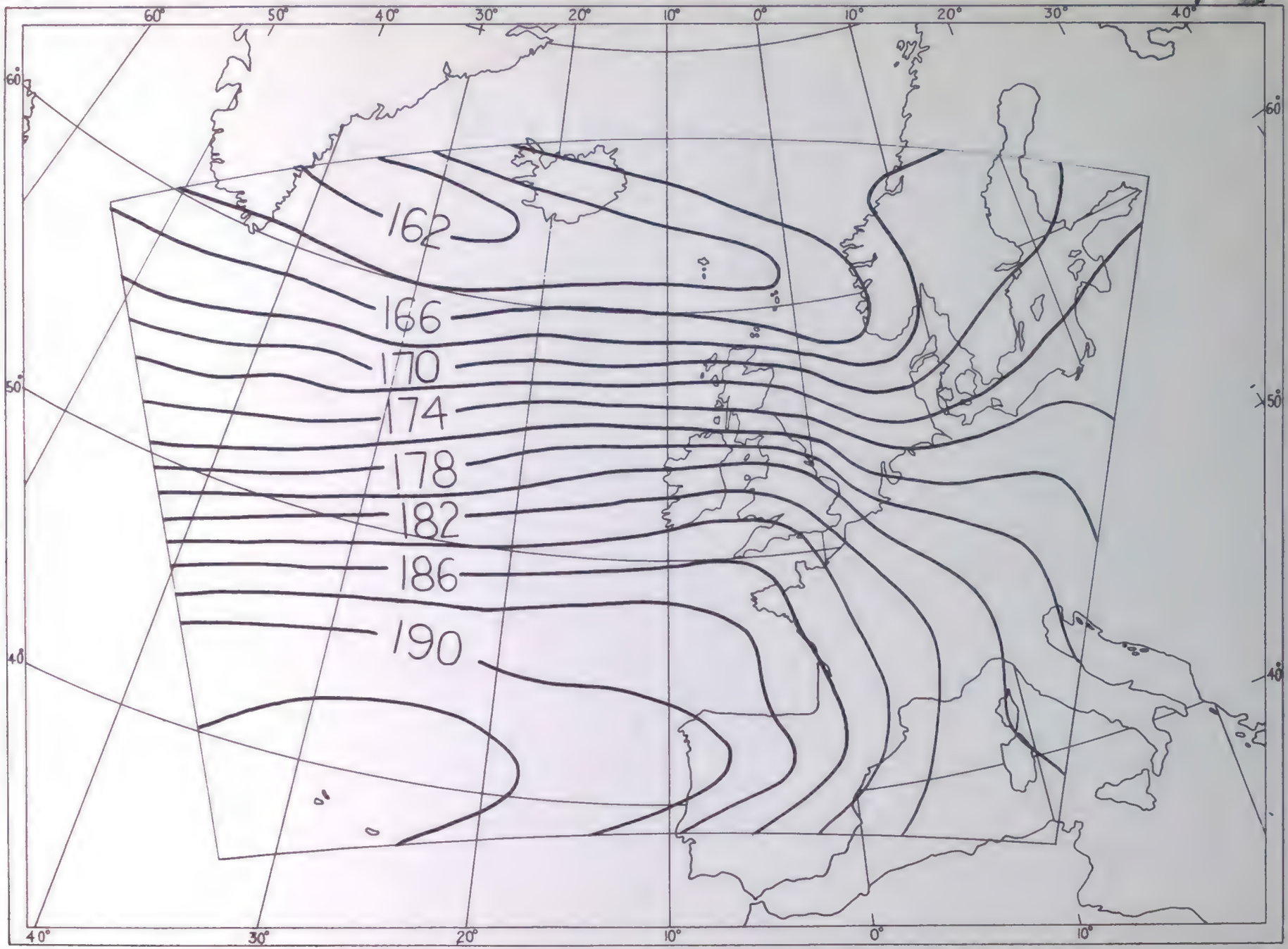


Fig 2(e) Computed 500mb. contour chart for 1500 G.M.T. 31:1:52

M.R.P. 956

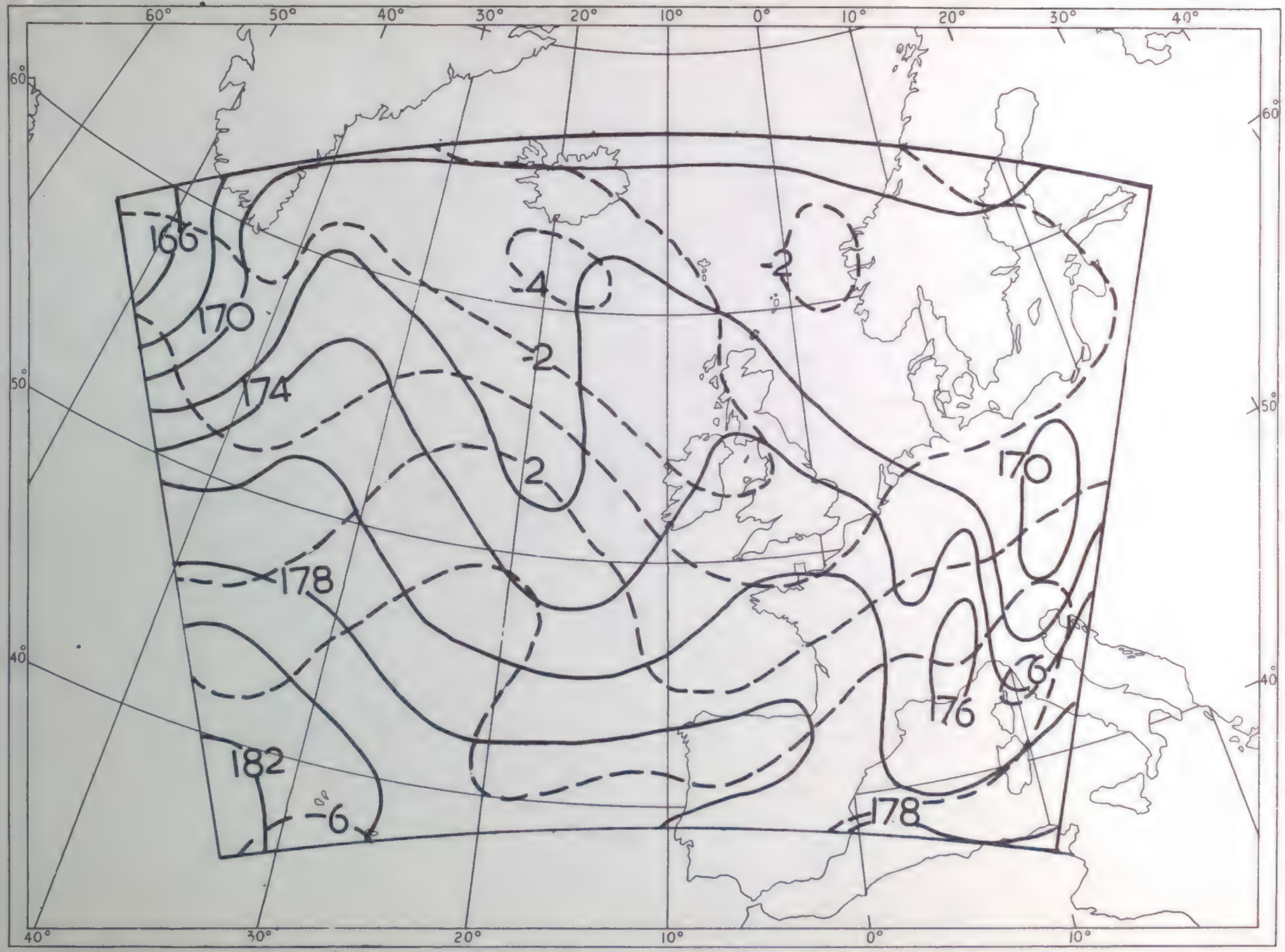


Fig.1(f) Computed 1000-500 mb. thickness and 1000 mb. contour charts for 1500 G.M.T. 28:1:52

M.R.P. 956

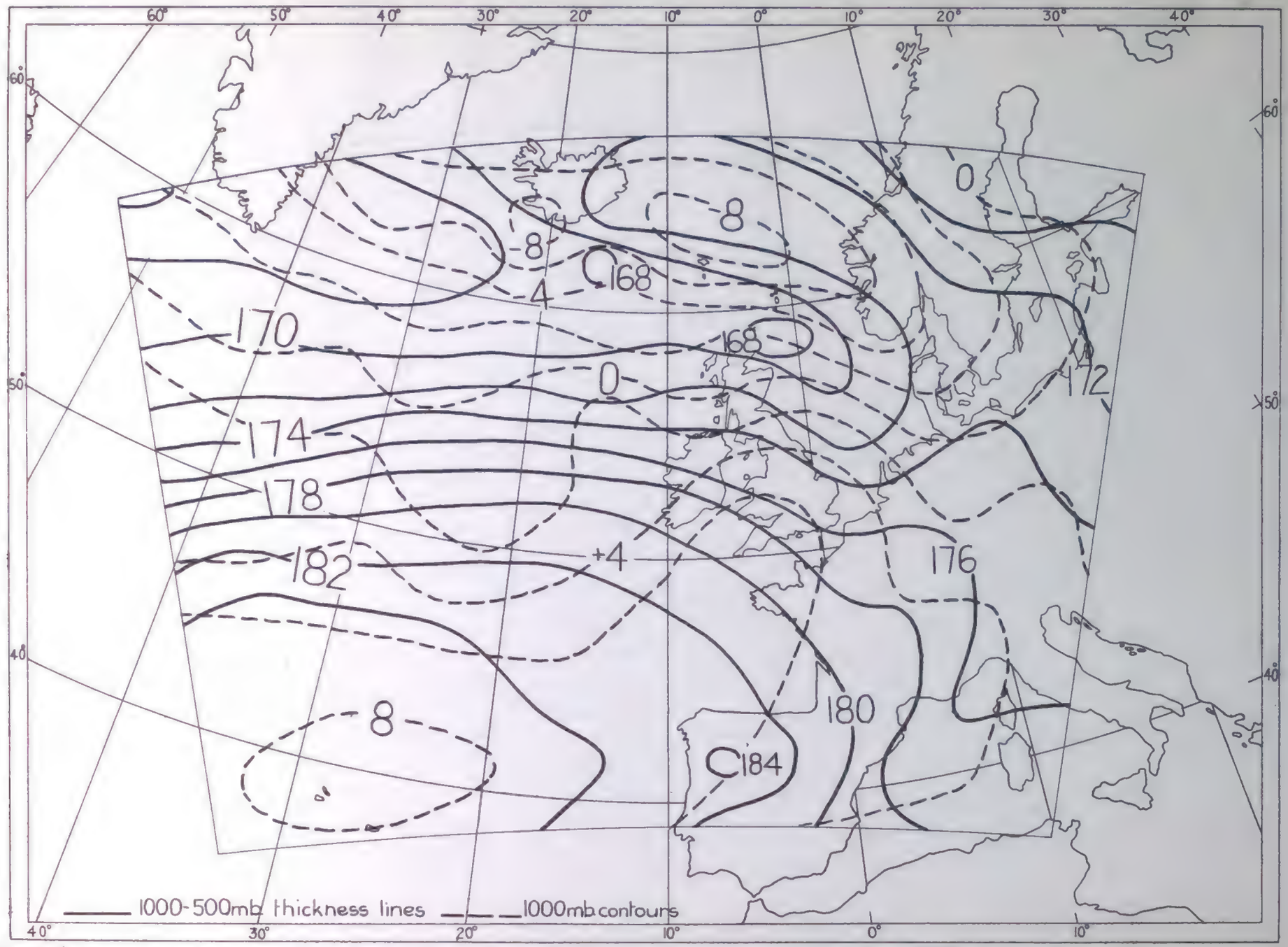


Fig 2(f) Computed 1000-500mb. thickness and 1000mb. contour charts for 1500 G.M.T. 31:1:52

M.R.P. 956

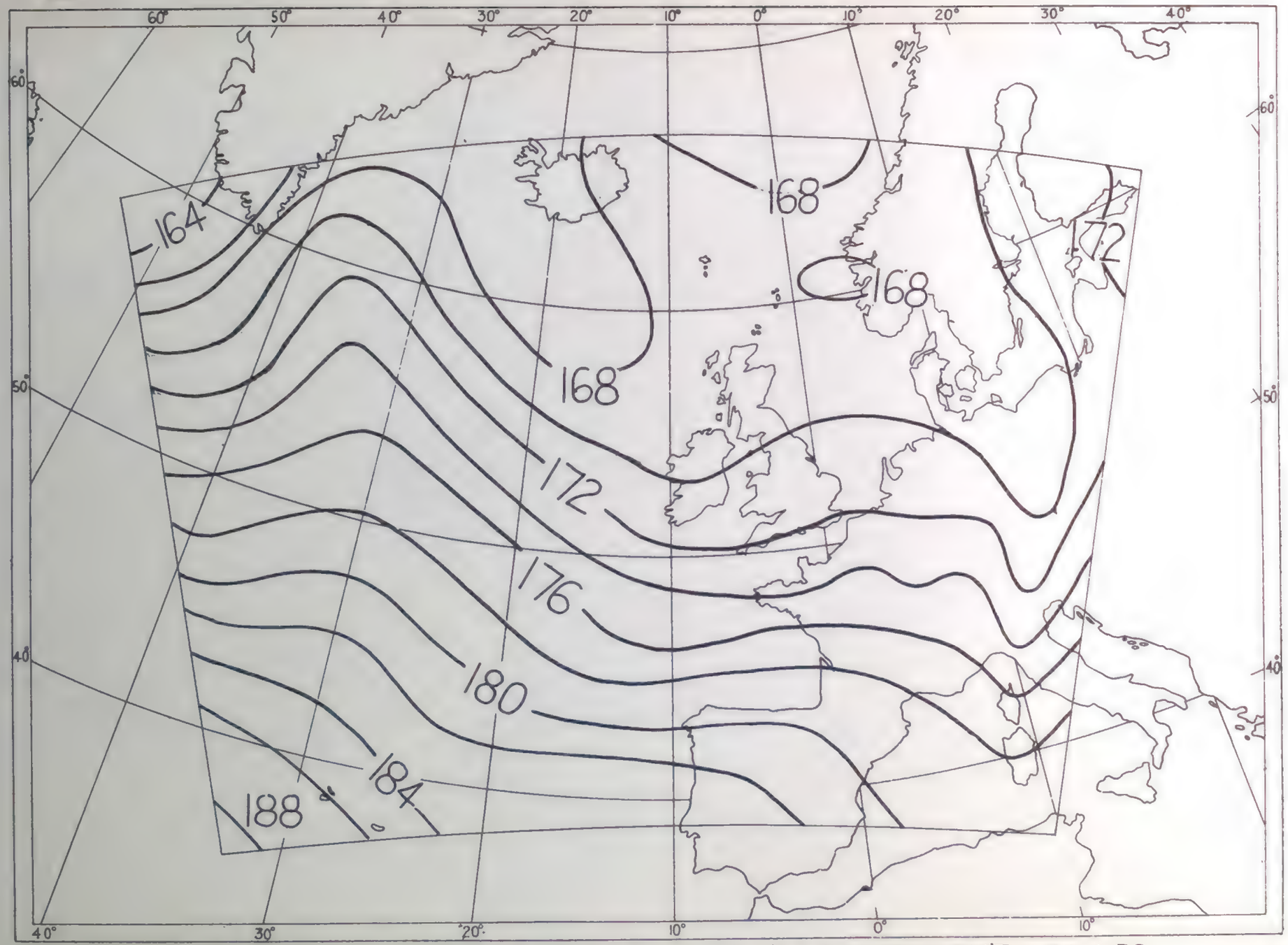


Fig 1(g) Computed 500mb. contour chart (using stream function) for 1500 G.M.T. 28:1:52

M.R.P. 956

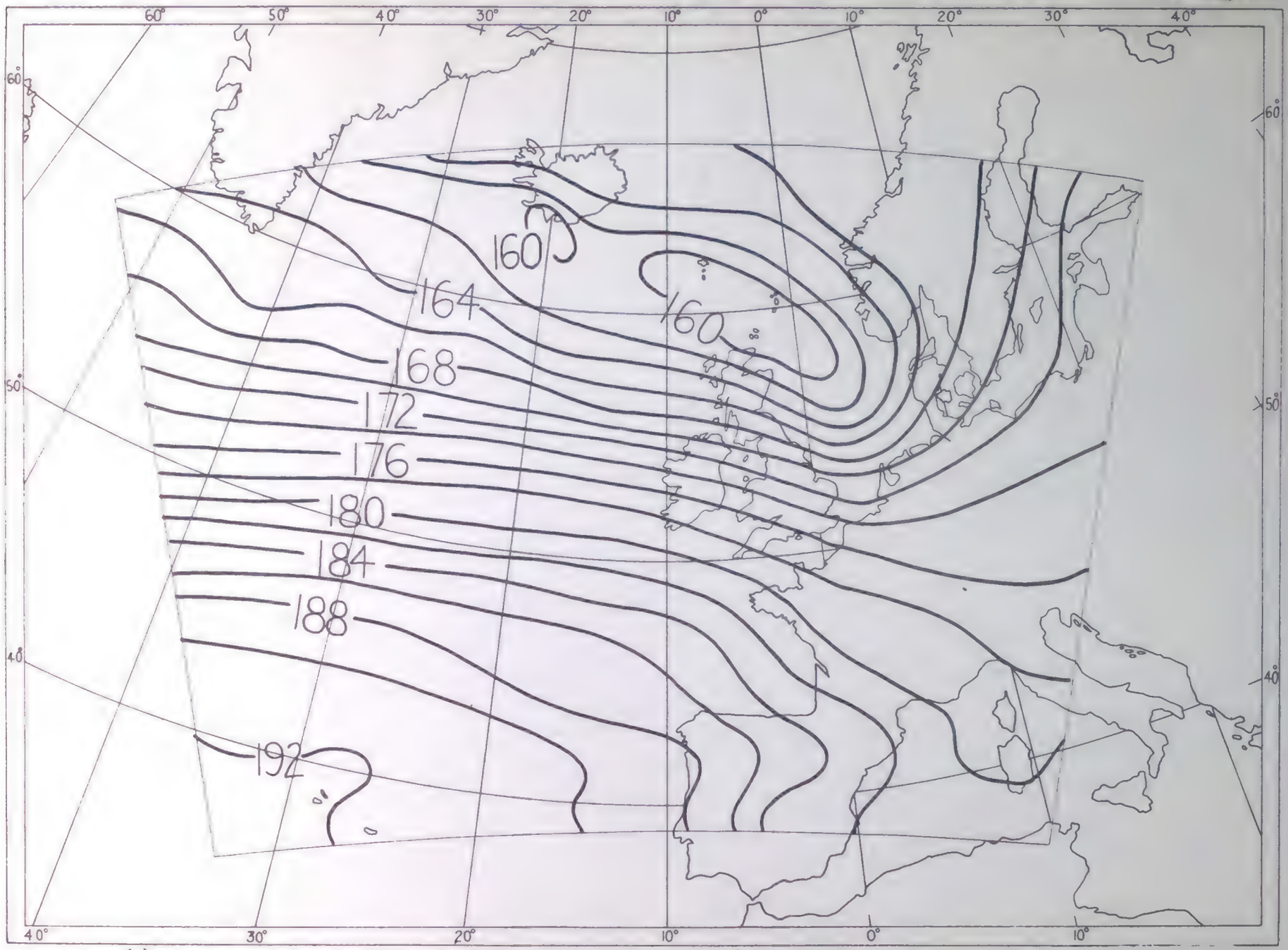


Fig 2(g) Computed 500mb. contour chart (using stream function) for 1500GM.T. 31:1:52

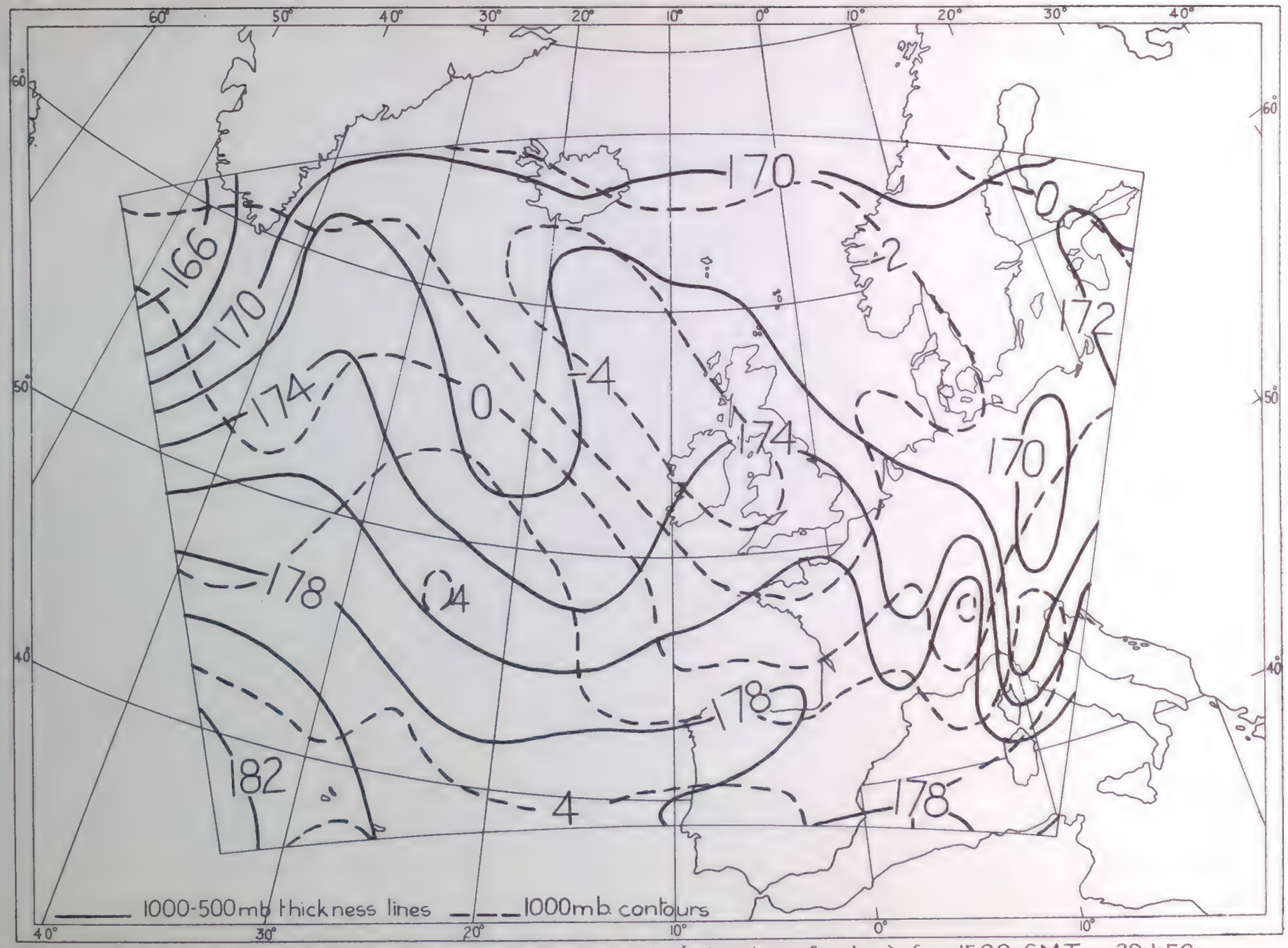


Fig 1(h). Computed 1000-500mb thickness and 1000mb contour charts (using stream function) for 1500 G.M.T. 28:1:52.

M.R.P. 956

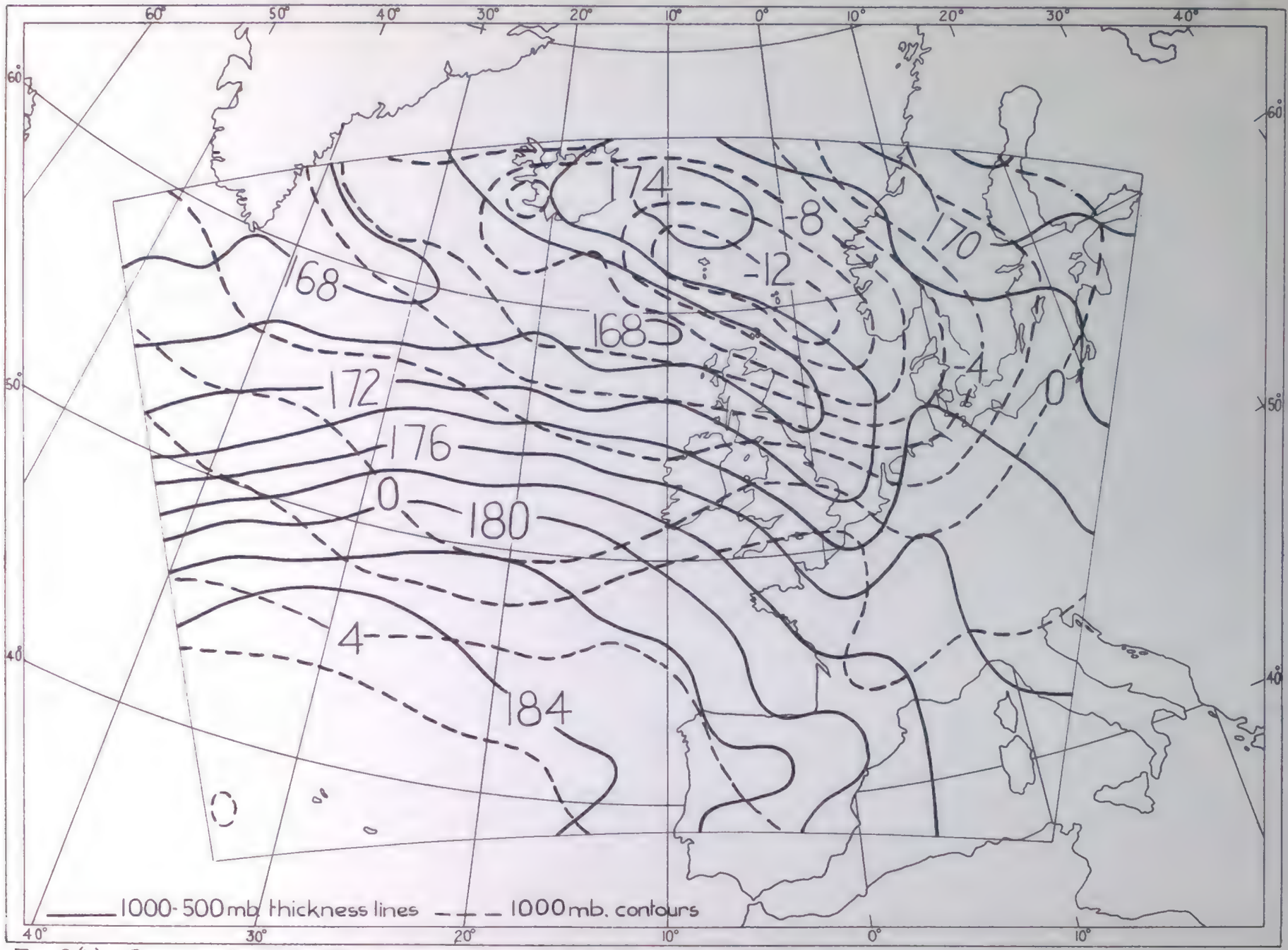


Fig 2(h) Computed 1000-500mb. thickness and 1000mb. contour charts (using stream function) for 1500 G.M.T. 31·1·52

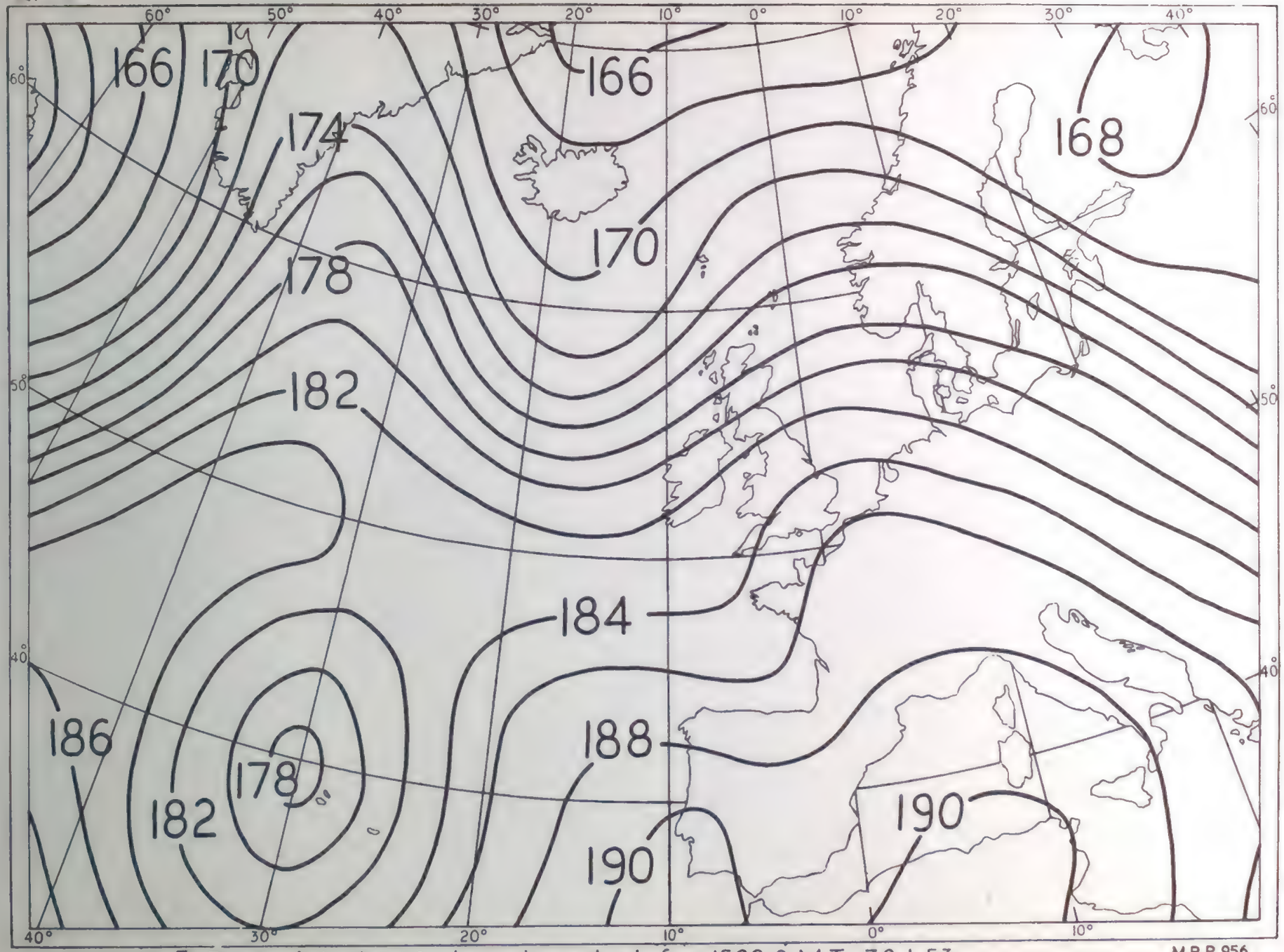


Fig.3(a) Actual 500mb. contour chart for 1500 G.M.T. 30.1.53

M.R.P. 956

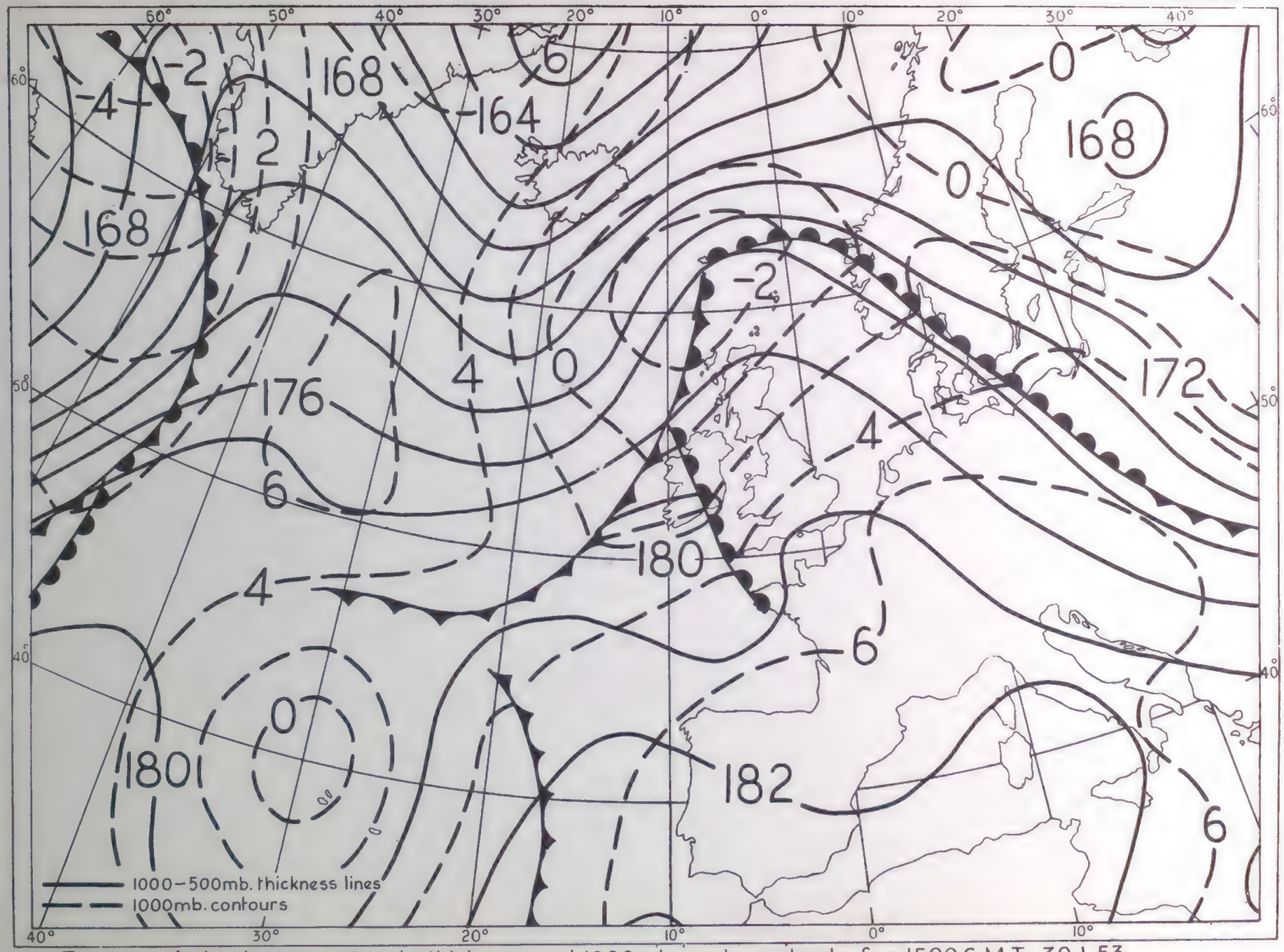


Fig.3(b) · Actual 1000–500mb. thickness and 1000mb. contour charts for 1500 G.M.T. 30.1.53

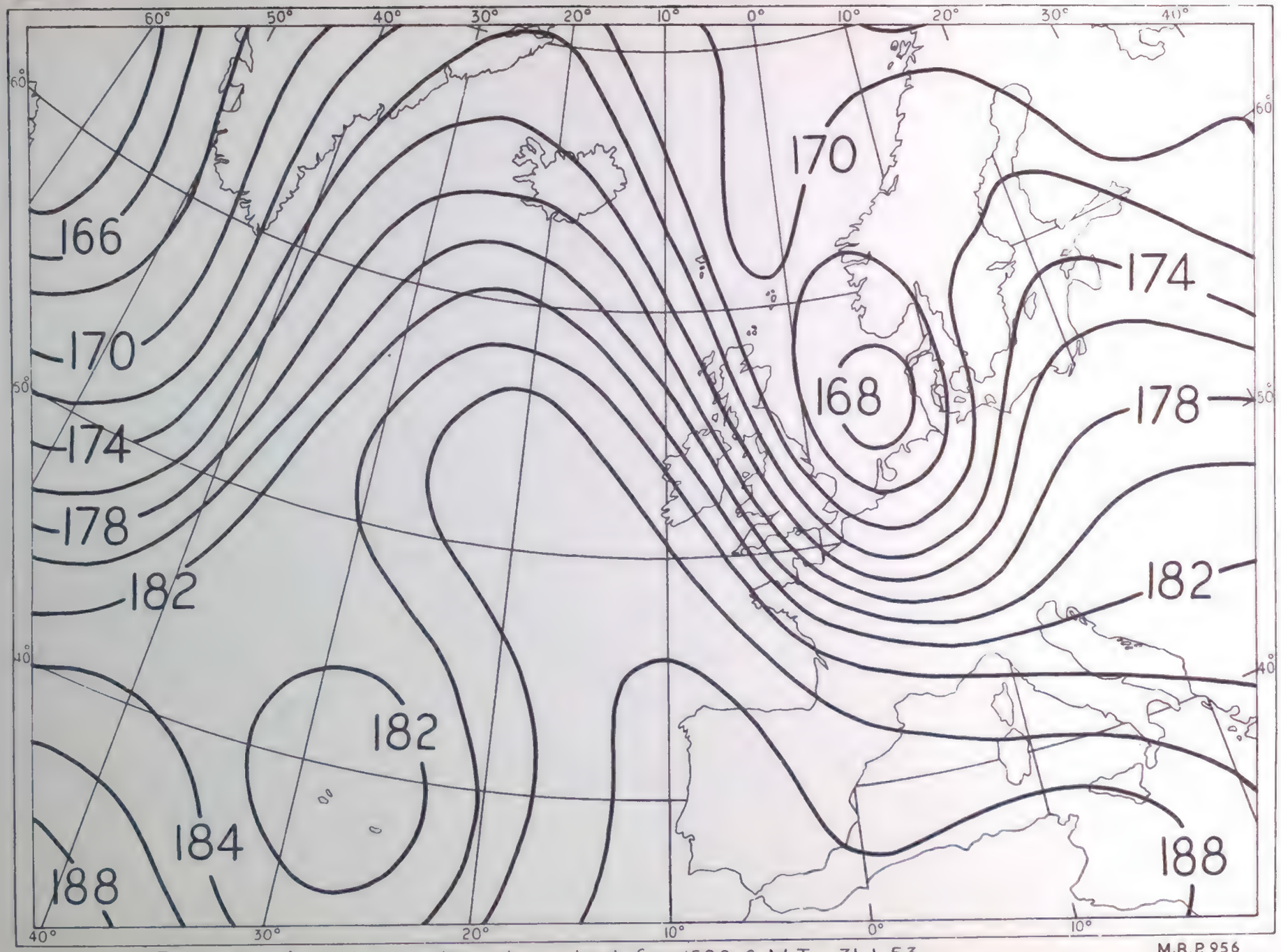


Fig. 3(c) Actual 500mb. contour chart for 1500 G.M.T. 31.1.53

M.R.P. 956

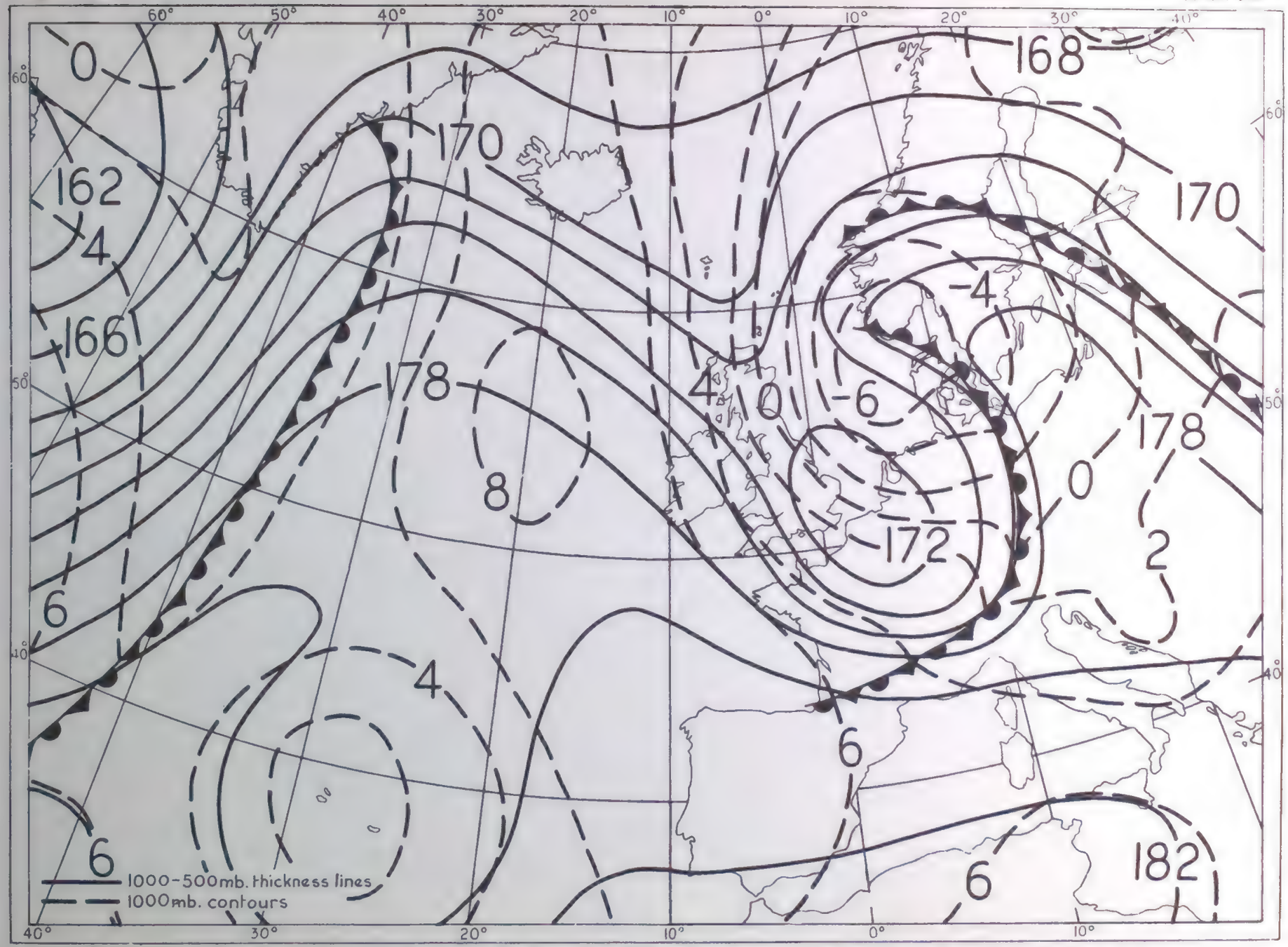


Fig. 3(d) Actual 1000-500mb. thickness and 1000mb. contour charts for 1500 G.M.T. 31.1.53

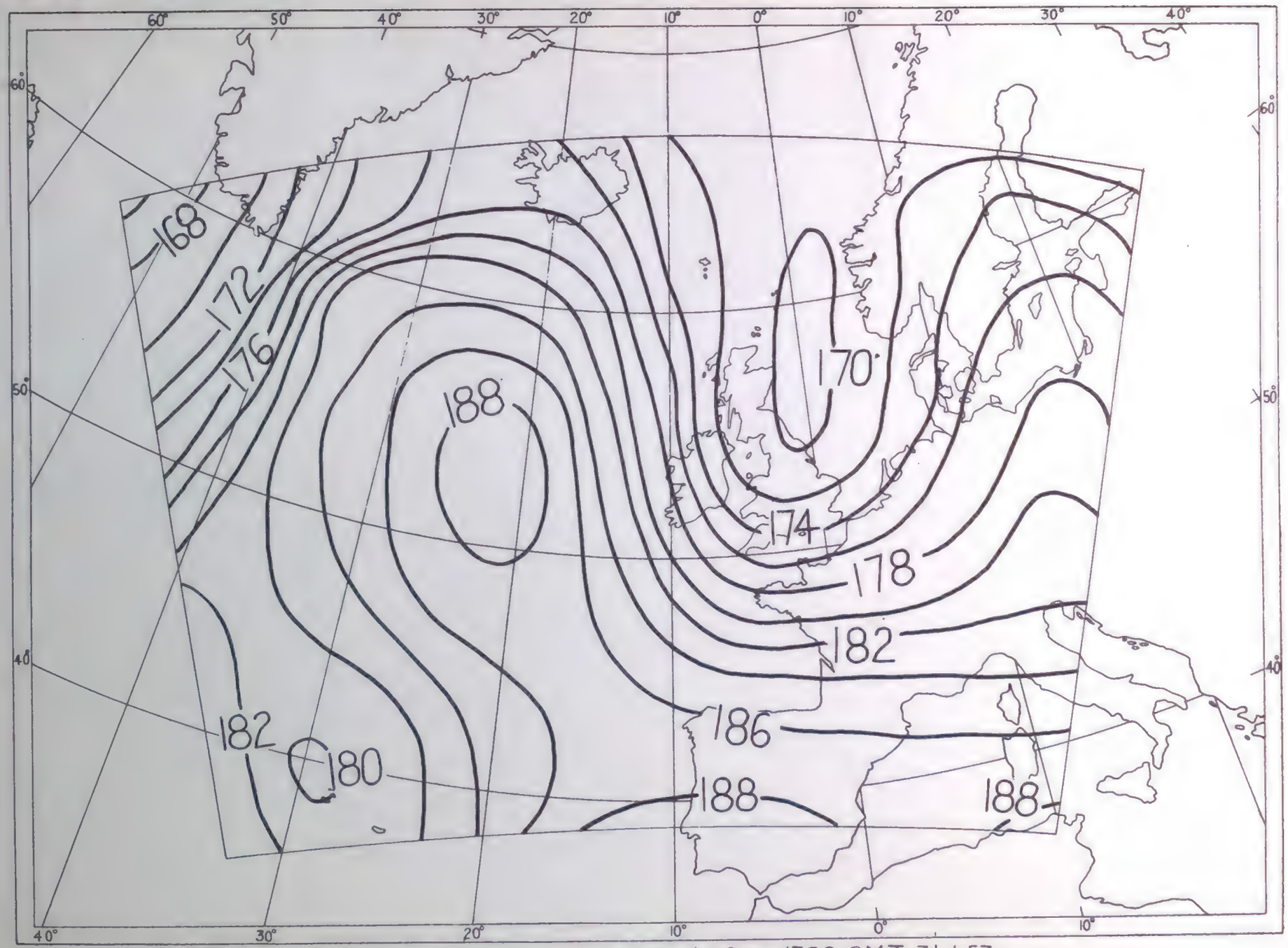


Fig. 3(e) Computed 500mb. contour chart for 1500 G.M.T. 31:1:53

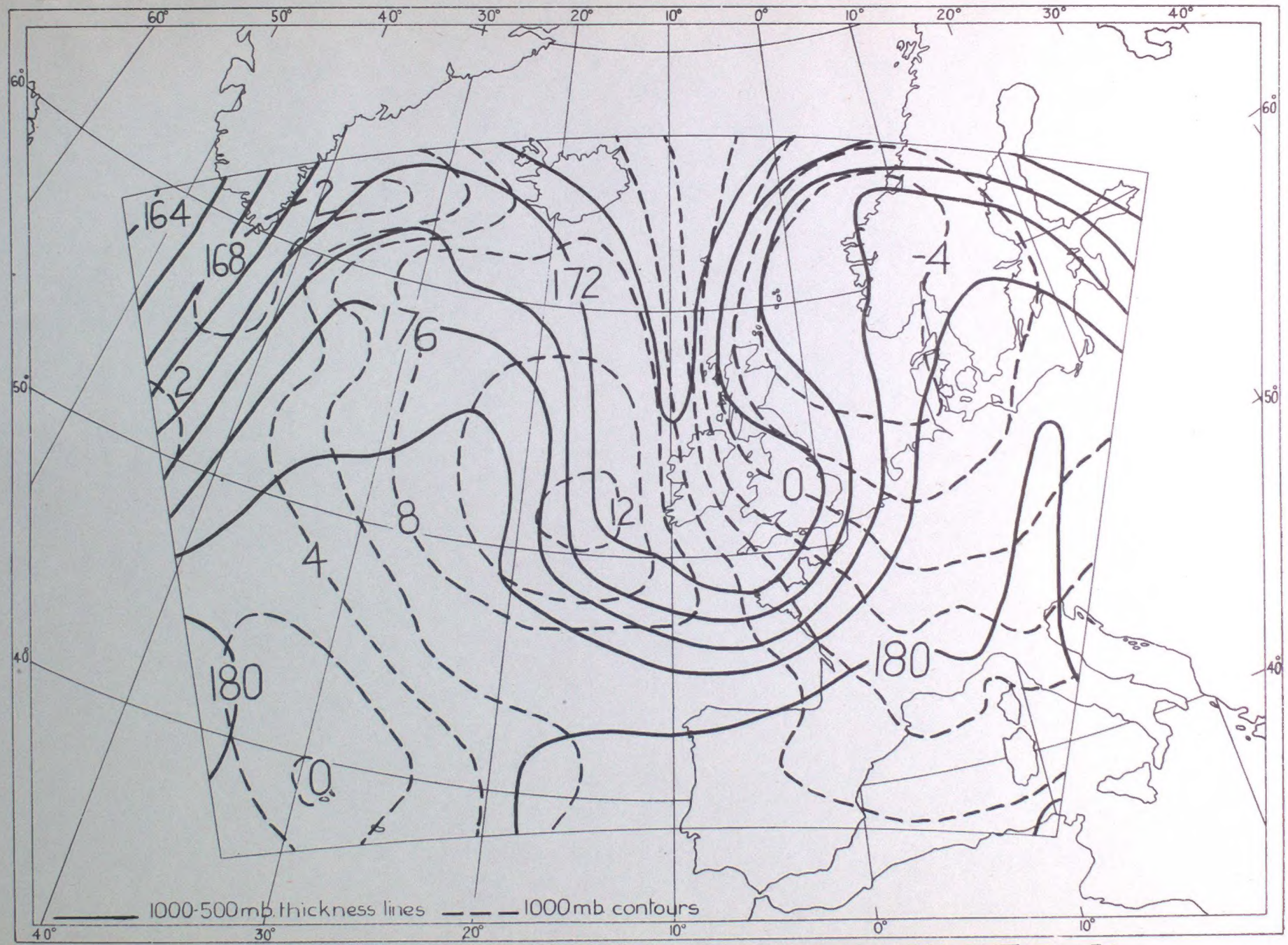


Fig.3(f) Computed 1000-500 mb. thickness and 1000 mb. contour charts for 1500 G.M.T. 31:1:53

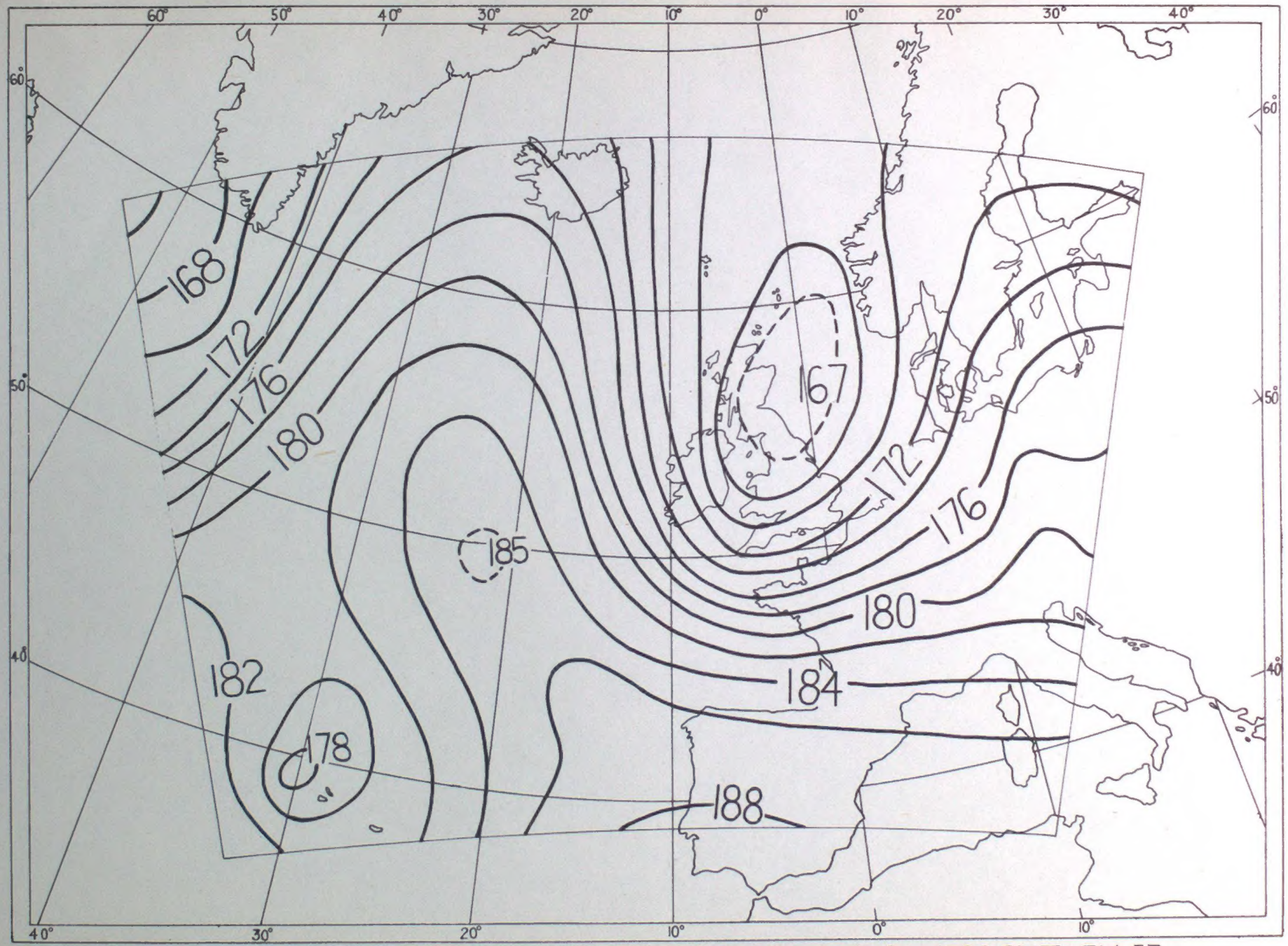


Fig. 3(g) Computed 500 mb. contour chart (using stream function) for 1500 G.M.T. 31:1:53

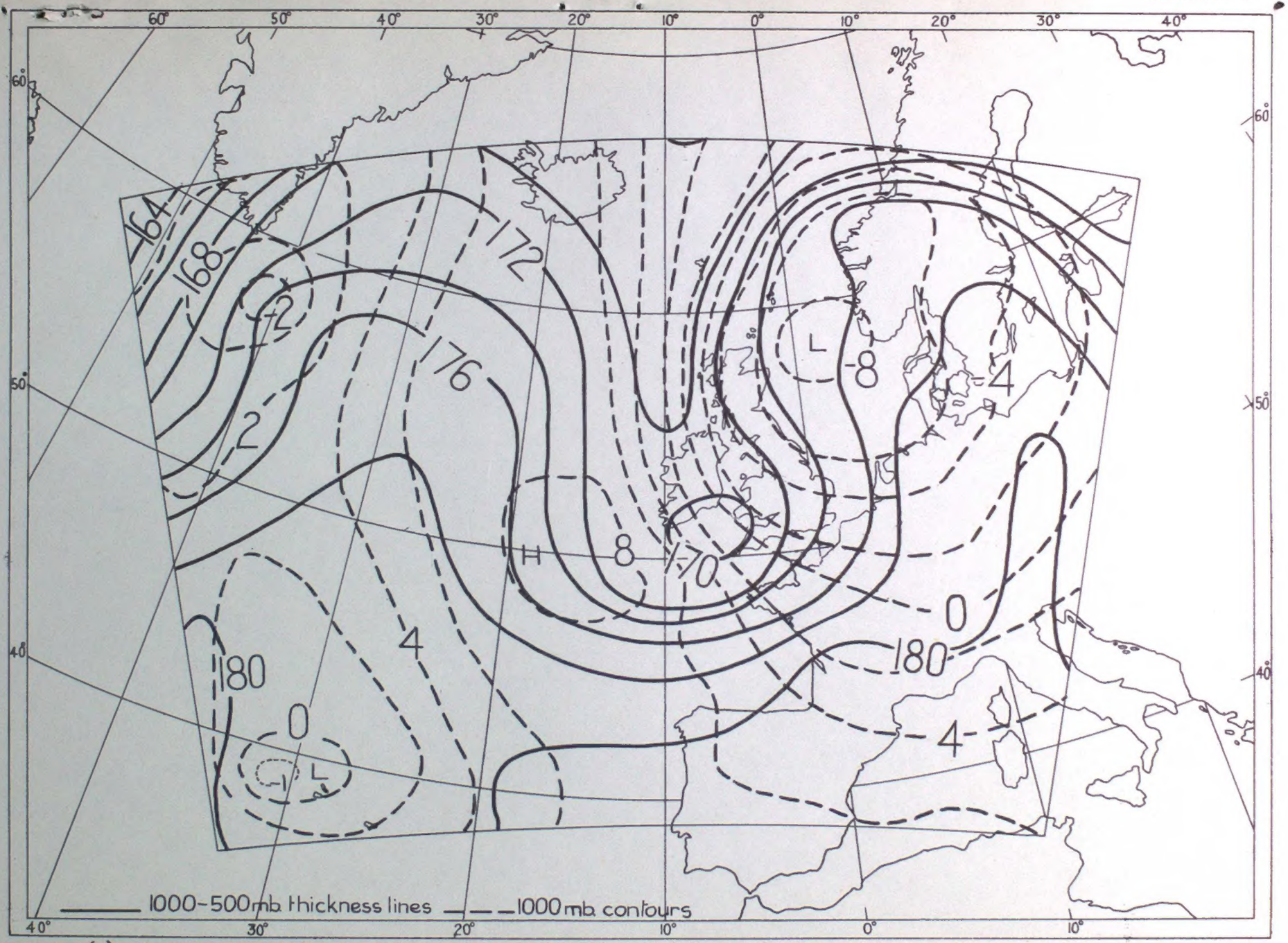


Fig. 3(h) Computed 1000-500mb. thickness and 1000mb. contour charts (using stream function) for 1500 G.M.T. 31:1:53

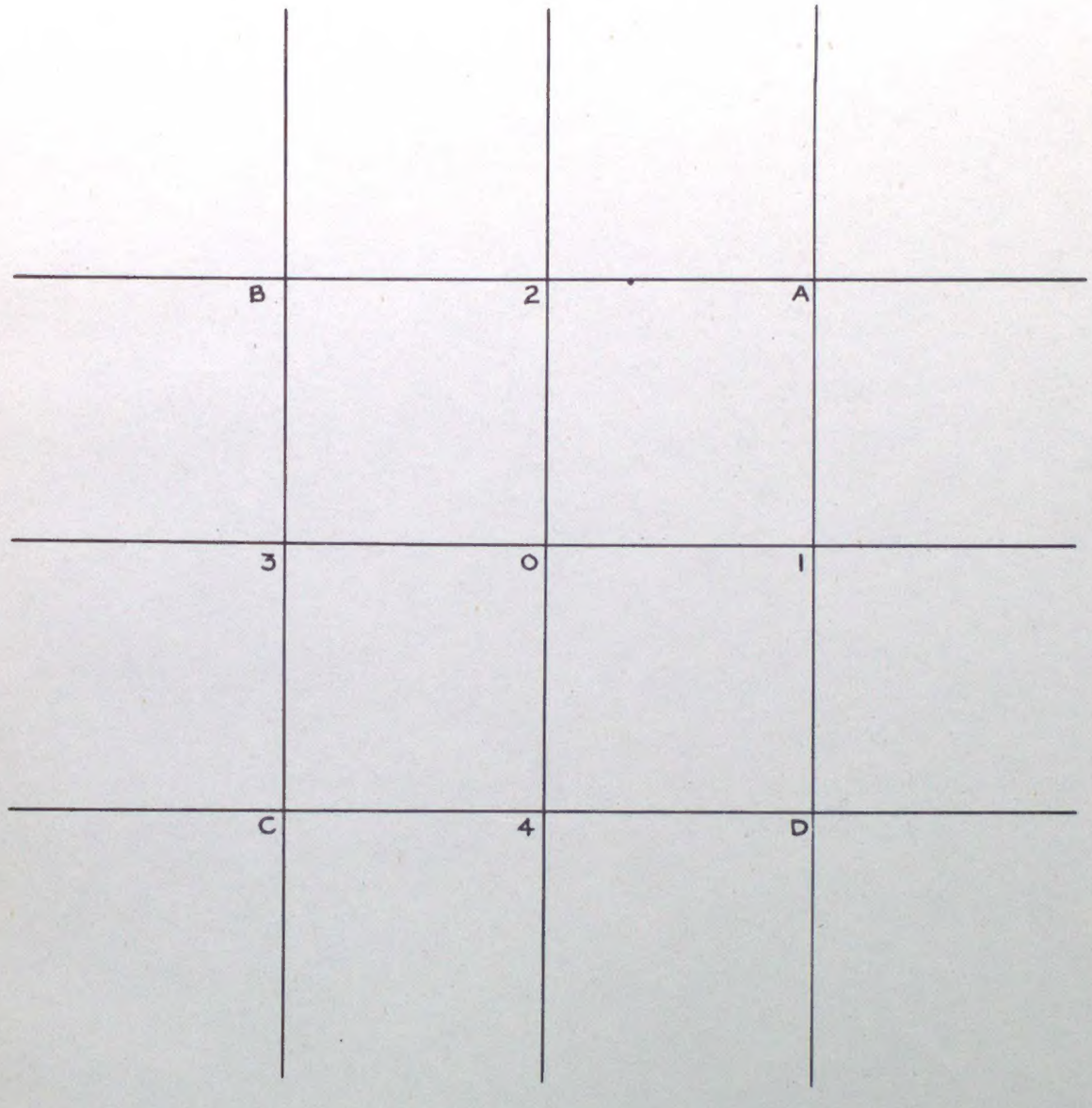


Fig.4

M.R.P. 956